SIAM J. Appl. Math.
Vol. 76, No. 1, pp. 110–137

A VARIATIONAL APPROACH TO THE INVERSE PHOTOLITHOGRAPHY PROBLEM*

LUCA RONDI†, FADIL SANTOSA‡, AND ZHU WANG§

Abstract. Photolithography is a process in the production of integrated circuits in which a mask is used to create an exposed pattern with a desired geometric shape. In the inverse problem of photolithography, a desired pattern is given and the mask that produces an exposed pattern which is close to the desired one is sought. We propose a variational approach formulation of this shape design problem and introduce a regularization strategy. The main novelty in this work is the regularization term that makes the thresholding operation involved in photolithography stable. The potential of the method is demonstrated in numerical experiments.

Key words. photolithograpy, shape optimization, inverse problem, calculus of variations, sets of finite perimeter, Γ-convergence

AMS subject classifications. 49Q10, 65N21, 49J45, 65K10

DOI. 10.1137/140991868

1. Introduction.

Photolithography is a key step in the production of integrated circuits. A detailed readable account of photolithography can be found in [11]. The book by Ma and Arce [5] gives a comprehensive introduction to the subject of lithography and presents several engineering approaches to the problem. Here we simply provide a brief description of the process in order to introduce the reader to the technology, and to quickly delve into the mathematical problem arising in photolithography.

Integrated circuits are created in layers. The circuit layout in each layer is made by first treating the substrate with a photo-resist. A pattern is transferred to the photo-resist using ultraviolet (UV) light and a mask. The UV light, diffracted by the mask, selects a pattern on the photo-resist that is to be removed. Once the pattern is removed, the substrate without the photo-resist is then etched.

The mask can be viewed as an opaque screen with cut-outs. UV light from a source goes through a system of lenses and is diffracted by the mask. The diffracted light creates an image on the photo-resist which is placed at the focal distance from the lenses. The photo-resist is light sensitive. Parts that are exposed to light intensity greater than some threshold can be removed.

For the purpose of this work, we call the pattern we wish to remove the "target pattern." For a given mask, the exposed pattern is the set of points on the photo-resist, where the UV light intensity is greater than some threshold. The inverse problem in photolithography is the problem of finding the mask that produces an

*Received by the editors October 17, 2014; accepted for publication (in revised form) October 27, 2015; published electronically January 14, 2016. This research was started at the Institute for Mathematics and Its Applications (IMA) when the third author was a postdoctoral fellow. The IMA receives funding from the NSF under Award DMS-0931945.

http://www.siam.org/journals/siap/76-1/99186.html

†Dipartimento di Matematica e Geoscienze, Università degli Studi di Trieste, 34127 Trieste, Italy (rondi@units.it). The research of this author was partially supported by Università degli Studi di Trieste through Fondo per la Ricerca di Ateneo—FRA 2012, and by GNAMPA, INdAM.

‡School of Mathematics, University of Minnesota, Minneapolis, MN 55455 (santosa@math.umn.edu). The research of this author was partially supported by NSF Award DMS-1211884.

§Department of Mathematics, University of South Carolina, Columbia, SC 29208 (wangzhu@math.sc.edu).

exposed pattern that is as close to the target pattern as possible. Such an inverse problem can be thought of as a shape design problem.

The mask is a set, and it may be represented by its characteristic function m, that is, by a binary function. Let $I = I(m)$ be the light intensity on the photo-resist plane for a given mask m. The exposed region is given by

$$\Omega(m) = \{x : \ I(x) > h\},$$

where h is the threshold. Thus $\Omega(m)$ is the suplevel set of the real valued function I at level h. Such a thresholding operation, besides being highly nonlinear, is not stable, for instance, with respect to variations of the threshold value h, in particular from the topological point of view, whenever h is close to a critical value for I. Notice that in order to describe Ω we can use again its characteristic function, namely,

$$\chi_\Omega = \mathcal{H}(I - h),$$

where $\mathcal{H}$ is the Heaviside function. The fact that $\mathcal{H}$ is not differentiable is another issue that has to be taken into account for the numerics.

Finally, the operator that maps the mask to the corresponding light intensity on the photo-resist plane is smoothing, and therefore a perfect agreement with the target pattern might be impossible, especially if it has some corners. This is the reason why we set the problem as an optimal design problem.

As described in [5], the first approaches to mask design were rule-based. The designers came up with certain rules to account for light diffraction. This type of approach quickly became inadequate as circuit size became smaller. Cobb [3] was the first to tackle this problem from the point of view of optimal design, using a physically based model. In his approach, diffraction is modeled by Kirchhoff approximation, which we also use here. The geometry of the cut-outs was constrained to move in a somewhat restricted manner. The geometry was varied in order to minimize the mismatch between the target pattern and the exposed pattern. The mismatch measure is the sum of distances at specified control points.

In works that followed, many of which are mentioned in [2], it was recognized that one can view the mask as a binary image. This realization allowed for variational formulations of the photolithography problem as well as representation of the desired binary image. The main issues are the choice of norms in which to measure the mismatch between the target and the exposed patterns, the representation of the unknown binary function, and the optimization methods for minimization. Also under consideration were accompanying issues such as manufacturability and stability of the exposed image under perturbation of the optics and exposure threshold.

One popular approach for representing the unknown binary image is the level set method [12]. Another approach is to use the phase-field method to represent the unknown as described in [10]. In [9] the mask is modeled as a pixelated binary image. In these three works, variational formulations were proposed.

A mathematical analysis of the geometric design problem of photolithography was first given in [10] and is the starting point of the present work. Given a desired circuit Ω_0, we wish to find a mask m minimizing the distance, in a suitable sense, of $\Omega(m)$ from Ω_0. In order for the mask to be constructed in a relatively easy way, we require that it not be too irregular, and therefore we add a perimeter penalization on the mask m. In [10] a suitable approximation, in the sense of Γ-convergence, of the resulting functional was proposed. Such an approximation was amenable to computation using, for example, finite difference approximations on structured grids and steepest descent

for minimization, and was based on approximating binary functions m by so-called phase-field functions u taking values in $[0, 1]$ and extending the intensity functional I to be defined not only on binary functions but also on phase-field functions. The approximation of the perimeter penalization used there was the one developed in this phase-field framework by Modica and Mortola [7]. We recall here that the same idea lies in the approximation of the Mumford–Shah functional due to Ambrosio and Tortorelli. Furthermore, also the Heaviside function was replaced by a smooth approximation.

In order to apply the analysis of [10], it is crucial that the threshold h not be a critical value of the intensity. In [10] this was obtained by imposing suitable technical restrictions on the model used. Instead, in this paper we greatly improve the results in [10] because we allow an extremely general model that includes the one usually used in the industry which is based on the so-called Hopkins aerial intensity representation. In fact, we are able to carry over the analysis by adding a further penalization term, which is the main theoretical novelty of this work. Such a regularization term, which we call $\mathcal{R}$ and is applied to the intensity I, has the aim of penalizing critical points at values close to the threshold and has two important effects. From the theoretical point of view, it allows the development of the analysis, and, from the practical point of view, it allows the reconstruction to be more stable, especially from the topological point of view, with respect to variations of the threshold, that is with respect to errors in the evaluation of the threshold value.

Using the approximation developed in [10] for the distance, the perimeter penalization, and the Heaviside function, and devising a suitable approximation for the regularization term $\mathcal{R}$, we construct an approximated functional which is still amenable to computation. The main theoretical result is that such an approximated functional is a good approximation, in the Γ-convergence sense, of the functional to be minimized; see Theorem 3.12. Therefore it is enough to compute a minimizer of the approximated functional, with the approximating parameter ε small enough, to have a good approximation of our solution. In order to show the validity of the method, we test it by numerical experiments. In our numerical tests we therefore look for a minimizer of one of these approximated functionals, with ε small enough. We employ a gradient method and therefore compute its gradient, at least in a discretized version of it. Unfortunately these functionals are highly nonconvex, and therefore a gradient method might lead to local instead of global minima. On the other hand, local minima might be occasionally difficult to avoid. Moreover, we wish to point out that our tests have the purpose of illustrating the potential of the method, and we do not aim for a more sophisticated numerical analysis of it. Our numerical tests show that the method performs rather well, leading to reconstructed circuits that are good approximations of the desired ones.

We point out important similarities and differences between our formulation and that of Choy et al. [2]. They considered a regularization term for the mask similar to the Modica–Mortola functional used in [10] and here as well. Another similarity is the use of an approximation of the Heaviside function in thresholding the image intensity to obtain the exposed pattern. It is important to note that our distance measure between the target and the exposed patterns given in (3.7) is different. Choy et al. focused on manufacturability, which is embodied in seeking masks that are close to the target pattern and whose total variation is small. Additionally they included a total variation penalty on the image intensity to improve stability to exposure threshold. In our work, we introduce the regularization $\mathcal{R}$ for stability. The effect

of this regularization is to move the critical points of the image intensity away from the threshold. One aspect we do not consider but that is discussed in Choy et al. is the uncertainty in the source of light. It should be mentioned that their work mainly addresses the computational issue. Moreover, a simplified model of image formation was used. Our work, on the other hand, has a theoretical foundation.

Our analysis and numerical experiments show that the terms introduced by Choy et al. to enforce manufacturability and stability may not achieve the desired effects. Namely, we show that the assumption that the mask and the target are close can be too restrictive and that it is not necessary to bound the gradient of the intensity function (which will never be very great due to the smoothing properties of the intensity functional I). Rather, it is important to bound the gradient away from zero, at least when the intensity is close to the assigned threshold.

It should be pointed out that modern photolithography now includes phase-shifting masks, i.e., masks whose cut-outs are optical elements that can shift the phase of the incoming UV light [5]. This added degree of freedom is not addressed in this work but clearly deserves further analysis.

The plan of the paper is the following. After a brief discussion of the mathematical preliminaries in section 2, we introduce the inverse photolithography problem and develop our variational approach in section 3. In section 4 we present our numerical experiments. Final comments, conclusions, and discussions are in sections 5 and 6.

2. Mathematical preliminaries. The following notation will be used. For every $x \in \mathbb{R}^2$, we shall set $x = (x_1, x_2)$, where x_1 and $x_2 \in \mathbb{R}$. For every $x \in \mathbb{R}^2$ and $r > 0$, we shall denote by $B_r(x)$ the open ball in $\mathbb{R}^2$ centered at x of radius r. Usually we shall write B_r instead of $B_r(0)$. For any set $E \subset \mathbb{R}^2$, we denote by χ_E its characteristic function, and for any $r > 0$, $B_r(E) = \bigcup_{x\in E} B_r(x)$.

For any $f \in \mathcal{S}'(\mathbb{R}^2)$, the space of tempered distributions, we denote by $\hat{f}$ its *Fourier transform*, which, if $f \in L^1(\mathbb{R}^2)$, may be written as

$$\hat{f}(\xi) = \int_{\mathbb{R}^2} f(x)\mathrm{e}^{-\mathrm{i}\xi\cdot x}\mathrm{d}x, \quad \xi \in \mathbb{R}^2.$$

We recall that $f(x) = (2\pi)^{-2}\hat{\hat{f}}(-x)$, that is, when also $\hat{f} \in L^1(\mathbb{R}^2)$,

$$f(x) = \frac{1}{(2\pi)^2}\int_{\mathbb{R}^2} \hat{f}(\xi)\mathrm{e}^{\mathrm{i}\xi\cdot x}\mathrm{d}\xi, \quad x \in \mathbb{R}^2.$$

For any function f defined on $\mathbb{R}^2$ and any positive constant s, we denote $f_s(x) = s^{-2}f(x/s)$, $x \in \mathbb{R}^2$. We note that $\|f_s\|_{L^1(\mathbb{R}^2)} = \|f\|_{L^1(\mathbb{R}^2)}$ and $\widehat{f_s}(\xi) = \hat{f}(s\xi)$, $\xi \in \mathbb{R}^2$.

By $\mathcal{H}^1$ we denote the 1-dimensional Hausdorff measure, and by $\mathcal{L}^2$ we denote the 2-dimensional Lebesgue measure. We recall that if $\gamma \subset \mathbb{R}^2$ is a smooth curve, then $\mathcal{H}^1$ restricted to γ coincides with its arclength. For any Borel $E \subset \mathbb{R}^2$ we denote $|E| = \mathcal{L}^2(E)$.

Let $\mathcal{D}$ be a bounded open set contained in $\mathbb{R}^2$, with boundary $\partial\mathcal{D}$. We say that $\mathcal{D}$ has a *Lipschitz boundary* if for every $x = (x_1, x_2) \in \partial\mathcal{D}$ there exist a Lipschitz function $\varphi : \mathbb{R} \to \mathbb{R}$ and a positive constant r such that for any $y \in B_r(x)$ we have, up to a rigid transformation,

$$y = (y_1, y_2) \in \mathcal{D} \quad \text{if and only if} \quad y_2 < \varphi(y_1). \tag{2.1}$$

We note that $\mathcal{D}$ has a finite number of connected components, whereas $\partial\mathcal{D}$ is formed by a finite number of rectifiable Jordan curves, and therefore $\mathcal{H}^1(\partial\mathcal{D}) = \text{length}(\partial\mathcal{D}) < +\infty$.

For any integer $k = 0, 1, 2, \ldots$, any α, $0 < \alpha \leq 1$, and any positive constants r and L, we say that a bounded open set $\mathcal{D} \subset \mathbb{R}^2$ is $C^{k,\alpha}$ *with constants* r *and* L if for every $x \in \partial\mathcal{D}$ there exists a $C^{k,\alpha}$ function $\varphi : \mathbb{R} \to \mathbb{R}$, with $C^{k,\alpha}$ norm bounded by L, such that for any $y \in B_r(x)$, and up to a rigid transformation, (2.1) holds. We note that we shall often use the notation *Lipschitz* instead of $C^{0,1}$.

Let us fix three positive constants r, L, and R. For any integer $k = 0, 1, 2, \ldots$ and any α, $0 < \alpha \leq 1$, we denote by $\mathcal{A}^{k,\alpha}(r, L, R)$ the class of all bounded open sets that are contained in $B_R \subset \mathbb{R}^2$ and are $C^{k,\alpha}$ with constants r and L.

We recall some basic properties of functions of bounded variation and sets of finite perimeter. For a more comprehensive treatment of these subjects see, for instance, [1].

Given a bounded open set $\mathcal{D} \subset \mathbb{R}^2$, we denote by $BV(\mathcal{D})$ the Banach space of *functions of bounded variation*. We recall that $u \in BV(\mathcal{D})$ if and only if $u \in L^1(\mathcal{D})$ and its distributional derivative Du is a bounded vector measure. We endow $BV(\mathcal{D})$ with the standard norm as follows. Given $u \in BV(\mathcal{D})$, we denote by $|Du|$ the total variation of its distributional derivative, and we set $\|u\|_{BV(\mathcal{D})} = \|u\|_{L^1(\mathcal{D})} + |Du|(\mathcal{D})$.

We say that a sequence of $BV(\mathcal{D})$ functions $\{u_h\}_{h=1}^{\infty}$ *weakly* converges* in $BV(\mathcal{D})$ to $u \in BV(\mathcal{D})$ if and only if u_h converges to u in $L^1(\mathcal{D})$ and Du_h weakly* converges to Du in $\mathcal{D}$, that is,

$$\lim_h \int_{\mathcal{D}} v \mathrm{d}Du_h = \int_{\mathcal{D}} v \mathrm{d}Du \quad \text{for any } v \in C_0(\mathcal{D}). \tag{2.2}$$

We recall that if a sequence of $BV(\mathcal{D})$ functions $\{u_h\}_{h=1}^{\infty}$ is bounded in $BV(\mathcal{D})$ and converges to u in $L^1(\mathcal{D})$, then $u \in BV(\mathcal{D})$ and u_h converges to u weakly* in $BV(\mathcal{D})$.

We say that a sequence of $BV(\mathcal{D})$ functions $\{u_h\}_{h=1}^{\infty}$ *strictly converges* in $BV(\mathcal{D})$ to $u \in BV(\mathcal{D})$ if and only if u_h converges to u in $L^1(\mathcal{D})$ and $|Du_h|(\mathcal{D})$ converges to $|Du|(\mathcal{D})$. Indeed, for any $a > 0$,

$$d_{st}(u, v) = \int_{\mathcal{D}} |u - v| + a\big||Du|(\mathcal{D}) - |Dv|(\mathcal{D})\big| \tag{2.3}$$

is a distance on $BV(\mathcal{D})$ inducing the strict convergence. We also note that strict convergence implies weak* convergence.

We recall that if $\mathcal{D}$ is a bounded open set with Lipschitz boundary, then for any $C > 0$ the set $\{u \in BV(\mathcal{D}) : \|u\|_{BV(\mathcal{D})} \leq C\}$ is a compact subset of $L^1(\mathcal{D})$.

Let E be a bounded Borel set contained in $B_R \subset \mathbb{R}^2$. We shall denote by χ_E its characteristic function. We notice that E is compactly contained in B_{R+1}, which we shall denote by $E \Subset B_{R+1}$. We say that E is a *set of finite perimeter* if χ_E belongs to $BV(B_{R+1})$, and we call the number $P(E) = |D\chi_E|(B_{R+1})$ its *perimeter*.

Let us finally remark that the intersection of two sets of finite perimeter is still a set of finite perimeter. Moreover, whenever E is open and $\mathcal{H}^1(\partial E)$ is finite, E is a set of finite perimeter. In particular, a bounded open set $\mathcal{D}$ with Lipschitz boundary is a set of finite perimeter and its perimeter $P(\mathcal{D})$ coincides with $\mathcal{H}^1(\partial\mathcal{D})$.

We conclude this preliminary section by describing a classical Γ-convergence approximation of the perimeter functional due to Modica and Mortola [7]. For the definition and properties of Γ-convergence, we refer the reader to [4]. Throughout the paper, for any p, $1 \leq p \leq +\infty$, we shall denote its conjugate exponent by p', that is, $p^{-1} + (p')^{-1} = 1$.

THEOREM 2.1. *Let us fix* $R > 0$. *Let* $1 < p < +\infty$ *and* $W : \mathbb{R} \to [0, +\infty)$ *be a continuous function such that* $W(t) = 0$ *if and only if* $t \in \{0, 1\}$. *Let* $c_p = (\int_0^1 (W(s))^{1/p'} \mathrm{d}s)^{-1}$.

For any $\varepsilon > 0$ we define the functional $\mathcal{P}_\varepsilon : L^1(\mathbb{R}^2) \to [0, +\infty]$ as follows:

$$\mathcal{P}_\varepsilon(u) = \begin{cases} \dfrac{c_p}{p'\varepsilon}\displaystyle\int_{B_R} W(u) + \dfrac{c_p \varepsilon^{p-1}}{p}\int_{B_R} |\nabla u|^p & \text{if } u \in W_0^{1,p}(B_R), \\ & \quad u = 0 \text{ a.e. outside } B_R, \\ +\infty & \text{otherwise.} \end{cases} \tag{2.4}$$

Let $\mathcal{P} : L^1(\mathbb{R}^2) \to [0, +\infty]$ be such that

$$\mathcal{P}(u) = \begin{cases} |Du|(B_{R+1}) & \text{if } u \in BV(B_{R+1}),\ u \in \{0,1\} \text{ a.e.}, \\ & \quad u = 0 \text{ a.e. outside } B_R, \\ +\infty & \text{otherwise.} \end{cases} \tag{2.5}$$

Then $\mathcal{P} = \Gamma\text{-}\lim_{\varepsilon \to 0^+} \mathcal{P}_\varepsilon$ with respect to the $L^1(\mathbb{R}^2)$ norm.

Remark 2.2. We observe that $\mathcal{P}(u) = P(E)$ if $u = \chi_E$, where E is a set of finite perimeter contained in B_R and $\mathcal{P}(u) = +\infty$ otherwise.

Furthermore, we note that the result does not change if in the definition of $\mathcal{P}_\varepsilon$ we set $\mathcal{P}_\varepsilon(u) = +\infty$ whenever u does not satisfy the constraint

$$0 \le u \le 1 \text{ a.e. in } B_R. \tag{2.6}$$

Actually, in the numerics we shall always implicitly impose such a constraint.

Also, the following result due to Modica [6] will be useful.

PROPOSITION 2.3. *Let us consider any family $\{u_\varepsilon\}_{0<\varepsilon\le\tilde{\varepsilon}}$ such that for some positive constant C and for any ε, $0 < \varepsilon \le \tilde{\varepsilon}$, we have $0 \le u_\varepsilon \le 1$ almost everywhere and $\mathcal{P}_\varepsilon(u_\varepsilon) \le C$. Then $\{u_\varepsilon\}_{0<\varepsilon\le\tilde{\varepsilon}}$ is precompact in $L^1(\mathbb{R}^2)$.*

3. The inverse problem and its approximation. Kirchhoff approximation is currently favored as a modeling tool for the optical phenomena in photolithography. This is due to the fact that Kirchhoff approximation can be very efficiently computed and is relatively accurate. It is true, however, that more accurate optical modeling may be needed in the future. Under this approximation, the open portions of the mask act as light sources; the amplitude of light at the mask opening is that of the incident field from the light source. Propagation through the lenses can be calculated using Fourier optics. It is further assumed that the image plane, in this case the plane of the photo-resist, is at the focal distance of the optical system. If there were no diffraction, a perfect image of the mask would be formed on the image plane. Diffraction, together with partial coherence of the light source, acts to distort the formed image.

The mask, which consists of cut-outs, is represented as a binary function, the characteristic function of the cut-outs D. Namely, the mask is given by

$$m(x) = \chi_D(x).$$

The light intensity on the image plane is given by [8]

$$I(x) = \int_{\mathbb{R}^2}\int_{\mathbb{R}^2} m(\xi)K(x-\xi)J(\xi-\eta)\overline{K}(x-\eta)m(\eta)\mathrm{d}\xi\mathrm{d}\eta, \quad x \in \mathbb{R}^2. \tag{3.1}$$

In the above expression the kernel $K(\cdot)$ is called the *coherent point spread function* and describes the optical system. The function $J(\cdot)$ is called the *mutual intensity*

function. If the illumination is fully coherent, then $J \equiv 1$, but in practice illumination is never fully coherent. Equation (3.1) is often referred to as the Hopkins aerial intensity representation.

3.1. Assumptions on K and J. We assume that K is a complex valued function such that for a constant α, $0 < \alpha \leq 1$, we have $K \in C^{1,\alpha}(\mathbb{R}^2)$. Furthermore, we assume that $|K|$ converges to 0 uniformly as $\|x\| \to +\infty$; that is, for any $\varepsilon > 0$ there exists $r > 0$ such that for any $x \in \mathbb{R}^2$ with $\|x\| \geq r$ we have $|K(x)| \leq \varepsilon$.

We assume that J is the Fourier transform of a function $\hat{J}$ such that $\hat{J} \in L^1(\mathbb{R}^2)$ and $\hat{J} \geq 0$ almost everywhere in $\mathbb{R}^2$. In particular, J is a continuous complex valued function.

A typical model for K and J is the following. For an optical system with a circular aperture, once the wavenumber of the light used, $k > 0$, has been chosen, the kernel depends on a single parameter called the numerical aperture (NA). Notice that the wavelength is $\lambda = 2\pi/k$. Let us recall that the so-called Jinc function is defined as

$$\mathrm{Jinc}(x) = \frac{J_1(|x|)}{2\pi|x|}, \quad x \in \mathbb{R}^2,$$

where J_1 is the Bessel function of order 1. We notice that in the Fourier space,

$$\widehat{\mathrm{Jinc}}(\xi) = \chi_{B_1}(\xi), \quad \xi \in \mathbb{R}^2.$$

If we denote $s = (k\mathrm{NA})^{-1}$, then the kernel is usually modeled as

$$K(x) = \mathrm{Jinc}_s(x) = \frac{k\mathrm{NA}}{2\pi} \frac{J_1(k\mathrm{NA}|x|)}{|x|}, \quad x \in \mathbb{R}^2, \tag{3.2}$$

and therefore

$$\hat{K}(\xi) = \chi_{B_1}(s\xi) = \chi_{B_{1/s}}(\xi) = \chi_{B_{k\mathrm{NA}}}(\xi), \quad \xi \in \mathbb{R}^2.$$

If NA goes to $+\infty$, that is, $s \to 0^+$, then $\hat{K}$ converges pointwise to 1, and thus K approximates in a suitable sense the Dirac delta.

The mutual intensity function $J(\cdot)$ is parametrized by a *coherency coefficient* σ. A typical model for J is

$$J(x) = 2\frac{J_1(k\sigma\mathrm{NA}|x|)}{k\sigma\mathrm{NA}|x|} = \pi\mathrm{Jinc}(k\sigma\mathrm{NA}|x|), \quad x \in \mathbb{R}^2. \tag{3.3}$$

Thus,

$$\frac{1}{(2\pi)^2}\hat{J}(\xi) = \frac{1}{\pi(k\sigma\mathrm{NA})^2}\chi_{B_{k\sigma\mathrm{NA}}}(\xi), \quad \xi \in \mathbb{R}^2, \tag{3.4}$$

which, as $\sigma \to 0^+$, converges, in a suitable sense, to the Dirac delta. Therefore full coherence is achieved for $\sigma \to 0^+$. In fact, if $\sigma \to 0^+$, J converges to 1 uniformly on any compact subset of $\mathbb{R}^2$.

The photo-resist material responds to the intensity of the image. When intensity at the photo-resist goes over a certain threshold, it is then considered exposed and can be removed. Therefore, the exposed pattern, given a mask $m(x)$, is

$$\Omega = \{x \in \mathbb{R}^2 \,:\, I(x) > h\}, \tag{3.5}$$

where $h > 0$ is the exposure threshold. Clearly, Ω depends on the mask function $m(x)$, which we recall is given by the characteristic function of D representing the cut-outs, that is, $\Omega = \Omega(D)$. In photolithography, we have a desired exposed pattern Ω_0 that we wish to achieve. The inverse problem is to find a mask that achieves this desired exposed pattern, that is, to find D such that $\Omega(D) = \Omega_0$. Mathematically, this cannot, in general, be done. In fact the operator I is smoothing, and therefore $\Omega(D)$ would be, in general, smooth as well. This makes it almost impossible to reconstruct sharp corners, for instance. In our numerical experiments the reconstructed circuits present rounded corners exactly for this reason. Therefore, the inverse problem must be posed as an optimal design problem.

3.2. Assumptions on the target pattern Ω_0. Let us fix $R > 0$. We assume that Ω_0 is a bounded open set compactly contained in B_R such that Ω_0 is a set of finite perimeter.

Suppose the desired pattern is given by Ω_0. We pose the minimization problem

$$\min_{D \in \mathcal{A}} d(\Omega(D), \Omega_0). \tag{3.6}$$

Concerning the distance function $d(\cdot, \cdot)$ and the admissible set $\mathcal{A}$, we shall choose the following. We set

$$\mathcal{A} = \{E \subset B_R : \ E \text{ is a set of finite perimeter}\},$$

and for any $E \in \mathcal{A}$ we denote by $P(E)$ its perimeter and notice that

$$P(E) = \mathcal{P}(\chi_E),$$

where, for any function $u \in L^1(\mathbb{R}^2)$, $\mathcal{P}(u)$ is defined in (2.5). With a slight abuse of notation we shall identify sets with their characteristic functions, so that $\mathcal{A}$ may also denote

$$\mathcal{A} = \{u \in L^1(\mathbb{R}^2) : \ \mathcal{P}(u) < +\infty\}.$$

About the distance we shall choose

$$d(\Omega_1, \Omega_2) = d_{st}(\chi_{\Omega_1}, \chi_{\Omega_2}) = \int |\chi_{\Omega_1} - \chi_{\Omega_2}| + a|P(\Omega_1) - P(\Omega_2)|, \tag{3.7}$$

where a is a positive tuning parameter. We recall that in [10, section 3.3] the choice of the distance has been thoroughly discussed. Here we emphasize the role of the part containing the difference between the two perimeters. Such a term is a regularizing term. Assuming that Ω_1 is smooth, it essentially prevents Ω_2 from having a highly oscillating boundary or Ω_2 from presenting some thin and long spikes. In both cases the measure of the symmetric difference between Ω_1 and Ω_2, the first term in our distance, may be small but the difference between the two perimeters would be large. We notice that in our numerical tests, actually the difference between the two perimeters does not play a particularly important role. We believe this is due to the fact that the operator I is extremely smoothing, and this already provides the regularization effect that prevents oscillations or spikes, thus making superfluous adding the difference between the two perimeters in the distance.

We shall add to (3.6) two regularization terms. The first is on the independent variable D, that is, on the mask. To ensure manufacturing of the mask, the optimal

mask may not be too irregular, and therefore we shall add a perimeter penalization on the mask. The second regularization term allows us to stabilize the optimization procedure. In fact, the thresholding operation that, given the intensity, determines the target domain is not stable. For instance, if h is a critical value of the intensity I, a very small modification of the mask might lead to a change in the topology of the reconstructed circuit. In order to avoid this, we shall discard masks such that h is close to a critical value of the corresponding intensity I. We shall achieve this by adding a second penalization term $\mathcal{R}$, which we describe later in this section.

Let us set up the regularized minimization problem. We denote

$$A = \{u \in L^1(\mathbb{R}^2) : \ 0 \le u \le 1 \text{ a.e. in } \mathbb{R}^2 \text{ and } u = 0 \text{ a.e outside } B_R\}.$$

Let us define the operator $\mathcal{I} : A \to C^0(\mathbb{R}^2)$ such that for any $u \in A$ we have

$$\mathcal{I}(u)(x) = \int_{\mathbb{R}^2}\int_{\mathbb{R}^2} u(\xi)K(x-\xi)J(\xi-\eta)\overline{K}(x-\eta)u(\eta)\mathrm{d}\xi\mathrm{d}\eta, \quad x \in \mathbb{R}^2. \tag{3.8}$$

Let us note that if $u = \chi_D$ for a mask $D \subset B_R$, then $\mathcal{I}(u)$ coincides with the intensity I as defined in (3.1).

In the next proposition we describe some of the properties of $\mathcal{I}$.

PROPOSITION 3.1. *Under our assumptions on K and J, the following hold.*

(i) *For any $u \in A$, $\mathcal{I}(u)$ is a real valued function such that $\mathcal{I}(u) \ge 0$ in $\mathbb{R}^2$. Obviously, if u is identically equal to zero, then also $\mathcal{I}(u)$ is identically equal to zero.*

(ii) *For any $u \in A$, $\mathcal{I}(u) \in C^{1,\alpha}(\mathbb{R}^2)$, and, for any $R_1 > 0$, there exists $C > 0$ such that*

$$\|\mathcal{I}(u)\|_{C^{1,\alpha}(B_{R_1})} \le C \quad \textit{for any } u \in A.$$

(iii) *For any $R_1 > 0$, $\mathcal{I}$ is uniformly continuous with respect to the L^1 norm on A and the $C^{1,\alpha}$ norm on $C^{1,\alpha}(B_{R_1})$.*

(iv) *$\mathcal{I}(u)$ converges to 0 uniformly as $\|x\| \to +\infty$, uniformly with respect to $u \in A$; that is, for any $\varepsilon > 0$, there exists $r > 0$ such that for any $x \in \mathbb{R}^2$ with $\|x\| \ge r$ and any $u \in A$, we have $|\mathcal{I}(u)(x)| \le \varepsilon$.*

Proof. For any $u \in A$, we define $U \in L^1(\mathbb{R}^4)$ as follows:

$$U(x,y) = u(x)u(y)J(x-y) \quad \text{for any } x, y \in \mathbb{R}^2.$$

Then we define $H \in C^{1,\alpha}(\mathbb{R}^4)$ in the following way:

$$H(x,y) = K(x)\overline{K}(y) \quad \text{for any } x, y \in \mathbb{R}^2.$$

We notice that

$$\mathcal{I}(u)(x) = (H * U)(x,x) \quad \text{for any } x \in \mathbb{R}^2,$$

where $*$ denotes convolution, in this particular case in $\mathbb{R}^4$.

Therefore, parts (i), (iii), and (iv) follow immediately from standard properties of convolutions. Concerning (i), this requires a little more care. We call $T(u) = K * u$, where again $*$ denotes convolution, in this case in $\mathbb{R}^2$. Then, for any $k \in \mathbb{R}^2$, we denote $\tilde{u}_k(x) = u(x)\mathrm{e}^{\mathrm{i}k\cdot x}$ for any $x \in \mathbb{R}^2$. Then, for fixed $x \in \mathbb{R}^2$, we define the function

$$f(k) = |T(\tilde{u}_k)(x)|^2 = \int_{\mathbb{R}^2}\int_{\mathbb{R}^2} u(\xi)\mathrm{e}^{\mathrm{i}k\cdot\xi}K(x-\xi)\overline{K}(x-\eta)u(\eta)\mathrm{e}^{-\mathrm{i}k\cdot\eta}\mathrm{d}\xi\mathrm{d}\eta, \quad k \in \mathbb{R}^2.$$

Clearly $f(k)$ is nonnegative for any $k \in \mathbb{R}^2$, and therefore it would be enough to show that

$$\mathcal{I}(u)(x) = \frac{1}{(2\pi)^2} \int_{\mathbb{R}^2} \hat{J}(k) f(k) \mathrm{d}k,$$

and this follows simply by the Fubini theorem. □

Remark 3.2. We may replace the assumptions on J by the following and still have the previous proposition and the next results hold. We may assume that J is the Fourier transform of a tempered distribution $\hat{J}$ such that $\hat{J}$ has compact support and is semipositive definite, that is, $\langle \hat{J}, f \rangle \geq 0$ for any $f \in \mathcal{S}$ such that $f \geq 0$ everywhere in $\mathbb{R}^2$. We notice that again J is a continuous complex valued function, and therefore the proof of parts (ii), (iii), and (iv) is exactly the same. The argument for proving (i) is slightly more involved in this case, and we leave the details to the reader.

We denote by $\mathcal{H} : \mathbb{R} \to \mathbb{R}$ the Heaviside function such that $\mathcal{H}(t) = 0$ for any $t \leq 0$ and $\mathcal{H}(t) = 1$ for any $t > 0$. For any positive constant h, we set $\mathcal{H}_h(t) = \mathcal{H}(t - h)$ for any $t \in \mathbb{R}$. Then, fixing the threshold $h > 0$, we define $\mathcal{W} : A \to L^\infty(\mathbb{R}^2)$ as follows:

$$\mathcal{W}(u) = \mathcal{H}_h(\mathcal{I}(u)) \quad \text{for any } u \in A. \tag{3.9}$$

Clearly, for any $u \in A$, $\mathcal{W}(u)$ is the characteristic function of an open set, which we shall call $\Omega(u)$. That is,

$$\Omega(u) = \{x \in \mathbb{R}^2 \,:\, \mathcal{I}(u)(x) > h\} \quad \text{for any } u \in A. \tag{3.10}$$

In other words, $\chi_{\Omega(u)} = \mathcal{W}(u) = \mathcal{H}_h(\mathcal{I}(u))$. Moreover, whenever $u = \chi_E$, where E is a measurable subset of B_R, we shall denote $\Omega(E) = \Omega(\chi_E)$.

In order to define the regularization term $\mathcal{R}$, we need a few auxiliary functions. Let us fix a positive constant δ_0. Let $f : \mathbb{R} \to [0, +\infty]$ be a continuous function satisfying the following properties:

(i) f is identically equal to $+\infty$ on $(-\infty, 0]$,
(ii) f is decreasing,
(iii) f is identically equal to zero on $[\delta_0, +\infty)$,
(iv) the following behavior at 0 holds:

$$\lim_{s \to 0^+} f(s) s^{2/\alpha} \geq C > 0.$$

Let $\varphi : \mathbb{R} \to \mathbb{R}$ be a C^1 function such that

(i) $\varphi(h) > 0$,
(ii) φ is increasing before h and decreasing after h,
(iii) $\varphi(0) < -\delta_0$.

We notice that we can find positive constants δ and c_1 such that φ is greater than or equal to c_1 on $[h - \delta, h + \delta]$ and $\varphi(0) \leq -(\delta_0 + \delta)$.

For example, we may choose

$$f(s) = \mathrm{e}^{-\delta_0^2/(\delta_0^2 - s^2)} s^{-2/\alpha} \quad \text{for any } 0 < s < \delta_0, \tag{3.11}$$

with $f \equiv +\infty$ on $(-\infty, 0]$ and $f \equiv 0$ on $[\delta_0, +\infty)$, and

$$\varphi(s) = -a(s - h)^2 + b \quad \text{for any } s \in \mathbb{R}, \tag{3.12}$$

for suitable positive constants a and b. For instance, if we pick $a > 0$ and δ_0, $0 < \delta_0 \leq h/2$, such that $a\delta_0 \geq 1$, then we may take $\delta = c_1 = \delta_0$ provided b satisfies $\delta_0 + a\delta_0^2 \leq b \leq ah^2 - 2\delta_0$.

DEFINITION 3.3. *Let us define* $\mathcal{R} : A \to [0, +\infty]$ *as follows:*

$$\mathcal{R}(u) = \int_{\mathbb{R}^2} f\left(\|\nabla(\mathcal{I}(u))\|^2 - \varphi(\mathcal{I}(u))\right) \quad \text{for any } u \in A.$$

To get a sense of the behavior of the regularization term $\mathcal{R}$, consider a point x for which $\mathcal{I}(u(x)) \approx h$. This means that $\varphi(I(u)) > 0$. If $\|\nabla(\mathcal{I}(u(x)))\|$ is small, then $\mathcal{R} = +\infty$. The penalty term is zero if $\mathcal{I}(u(x))$ is relatively far from h. Therefore, the term $\mathcal{R}$ does not allow the critical values of $\mathcal{I}(u)$ to be close to h.

Remark 3.4. All the theoretical results we are going to prove remain valid if we replace $\mathcal{R}$ with $\tilde{\mathcal{R}} : A \to [0, +\infty]$ defined as follows:

$$\tilde{\mathcal{R}}(u) = \mathcal{R}(u) + \frac{1}{|\{h - \delta \leq \mathcal{I}(u) \leq h + \delta\}|} \quad \text{for any } u \in A.$$

PROPOSITION 3.5. *Under the previous notation and assumptions, we have that the functional* $\mathcal{R} : A \to [0, +\infty]$ *is continuous with respect to the* L^1 *convergence in* A.

Before proving Proposition 3.5, we need the following.

LEMMA 3.6. *Under the previous notation and assumptions, there exist positive constants* r, L, *and* $R_1 \geq R$ *such that for any* $u \in A$ *satisfying* $\mathcal{R}(u) < +\infty$, *and for any* $t \in [h - \delta, h + \delta]$, *we have that*

$$\Omega(t) = \{\mathcal{I}(u) > t\}$$

is either empty or belongs to $\mathcal{A}^{1,\alpha}(r, L, R_1)$.

Proof. Since $\mathcal{I}(u)$ decays to zero at infinity, uniformly with respect to $u \in A$, we observe that there exists $R_1 \geq R$ such that the following properties hold. First, $\{\mathcal{I}(u) \geq h - \delta\} \subset B_{R_1}$ for any $u \in A$. Moreover, if we denote

$$g(x) = \|\nabla \mathcal{I}(u)(x)\|^2 - \varphi(\mathcal{I}(u)(x)) \quad \text{for any } x \in \mathbb{R}^2,$$

we have that $g(x) \geq \delta_0$, and hence $f(g(x)) = 0$ for any $x \in \mathbb{R}^2$ with $\|x\| \geq R_1$ and any $u \in A$.

For fixed $u \in A$, let us define g as previously. By the continuity of g and the properties of f, if $\mathcal{R}(u)$ is finite, then $g(x)$ must be nonnegative for every $x \in \mathbb{R}^2$. This would be enough for the proof of this lemma, but actually we have that there exists a positive constant ε, depending on u, such that $g(x) \geq \varepsilon$ for every $x \in \mathbb{R}^2$. Since this property is crucial in the proof of Proposition 3.5, we sketch its proof here.

Since $g(x) \geq \delta_0$ for any x outside B_{R_1}, it would be enough to prove that $g(x) > 0$ for any $x \in \mathbb{R}^2$. We argue by contradiction and we assume that $g(x) = 0$ for some $x \in B_{R_1}$.

Then, since g is Hölder continuous with exponent α, $0 < \alpha \leq 1$, on the closure of B_{R_1+1}, we infer that for any y in a neighborhood of x we have that $g(y) \leq C|y - x|^\alpha$, and therefore by using polar coordinates centered at x we obtain, for some $r_0 > 0$,

$$\mathcal{R}(u) \geq 2\pi \int_0^{r_0} s f(Cs^\alpha) \mathrm{d}s.$$

Since the right-hand side is $+\infty$ by our assumptions on f, the claim is proved.

If $c_1 > 0$ is the minimum of φ on $[h-\delta, h+\delta]$, since $g(x) \geq 0$, we infer that

$$\|\nabla(\mathcal{I}(u))(x)\|^2 \geq c_1 \quad \text{if } \mathcal{I}(u)(x) \in [h-\delta, h+\delta].$$

Then the conclusion immediately follows by the uniform $C^{1,\alpha}$ regularity of $\mathcal{I}(u)$ proved in Proposition 3.1 and the implicit function theorem. □

Proof of Proposition 3.5. Let $u_n \in A$, $n \in \mathbb{N}$, converge to u in L^1 as $n \to \infty$. Clearly $u \in A$ as well.

We begin by considering the case in which $\mathcal{R}(u)$ is finite. In the previous lemma we proved that there exists a positive constant ε such that $g(x) \geq \varepsilon$ for any $x \in \mathbb{R}^2$. Since $\mathcal{I}(u_n)$ converges to $\mathcal{I}(u)$ locally in C^1 as $n \to \infty$, by the dominated convergence theorem we easily deduce that $\mathcal{R}(u_n)$ converges to $\mathcal{R}(u)$ as $n \to \infty$.

By the previous lemma, for any $u \in A$ such that $\mathcal{R}(u) < +\infty$ we have that $|\{h-\delta < \mathcal{I}(u) < h+\delta\}| = |\{h-\delta \leq \mathcal{I}(u) \leq h+\delta\}|$. By the uniform convergence of $\mathcal{I}(u_n)$ to $\mathcal{I}(u)$ as $n \to \infty$, and the dominated convergence theorem, we obtain that $|\{h-\delta \leq \mathcal{I}(u_n) \leq h+\delta\}|$ converges to $|\{h-\delta \leq \mathcal{I}(u) \leq h+\delta\}|$ as $n \to \infty$. Therefore, we immediately conclude that also $\mathcal{R}$ is continuous at any $u \in A$ such that $\mathcal{R}(u) < +\infty$.

If $\mathcal{R}(u) = +\infty$, then there exists x such that $g(x) \leq 0$. Consequently, if g_n is the corresponding function related to u_n, we conclude that $g_n(x)$ goes to zero as $n \to \infty$. Therefore

$$\mathcal{R}(u_n) \geq 2\pi \int_0^{r_0} s f(g_n(x) + Cs^\alpha) \mathrm{d}s \to +\infty \quad \text{as } n \to \infty,$$

and the proposition is proved. □

Let $\tilde{R} = R_1 + 1$ with R_1 as in Lemma 3.6. We notice that the functional $\mathcal{R}$ may be equivalently defined as

$$\mathcal{R}(u) = \int_{B_{\tilde{R}}} f\left(\|\nabla(\mathcal{I}(u))\|^2 - \varphi(\mathcal{I}(u))\right) \quad \text{for any } u \in A. \tag{3.13}$$

For any positive constant C, let us denote

$$\tilde{A}_C = \{u \in A : \ \mathcal{R}(u) \leq C\}.$$

LEMMA 3.7. *For any $C > 0$, the map $\mathcal{W} : \tilde{A}_C \to BV(B_{\tilde{R}})$ is uniformly continuous with respect to the L^1 norm on $\tilde{A}_C$ and the distance d_{st} on $BV(B_{\tilde{R}})$.*

Proof. By Lemma 3.6, we recall that, for any $u \in \tilde{A}_C$, $\mathcal{W}(u) = \chi_{\Omega(u)}$ where $\Omega(u)$ is either empty or belongs to $\mathcal{A}^{1,\alpha}(r, L, R_1)$. Then there exists a constant C_1 such that $d_{st}(\mathcal{W}(u), \mathcal{W}(v)) \leq C_1$ for any u and $v \in \tilde{A}_C$.

There exists a function $\omega : [0, +\infty) \to [0, +\infty)$, which is nondecreasing and such that $\lim_{t \to 0^+} \omega(t) = 0$, such that for any u and v belonging to A, we have

$$\|\mathcal{I}(u) - \mathcal{I}(v)\|_{L^\infty(B_{\tilde{R}})} \leq \omega(\|u - v\|_{L^1(\mathbb{R}^2)}).$$

We need the following claim.

CLAIM 1. *There exists a function $\tilde{g} : [0, +\infty) \to [0, +\infty)$, which is continuous, increasing, and such that $\tilde{g}(0) = 0$, satisfying the following property. For any $u \in \tilde{A}_C$ such that $\Omega(u)$ is not empty, for any $\varepsilon > 0$ and any $x \in \mathbb{R}^2$, we have*

$$\text{if } x \notin B_\varepsilon(\partial\Omega(u)), \text{ then } |\mathcal{I}(u)(x) - h| > \tilde{g}(\varepsilon). \tag{3.14}$$

To prove this claim, we recall that for a positive constant c_1 we have $\|\nabla(\mathcal{I}(u))(x)\| = -\nabla(\mathcal{I}(u))(x)\cdot\nu \geq \sqrt{c_1}$ for any $x \in \partial\Omega(u)$, where as usual ν is the outer normal to $\Omega(u)$. The $C^{1,\alpha}$ regularity of $\mathcal{I}(u)$ on $B_{\tilde{R}}$, which is uniform with respect to $u \in A$, allows us to conclude the proof of the claim.

We conclude that there exists a positive constant η_0 such that if u and $v \in \tilde{A}_C$ satisfy $\|u-v\|_{L^1(\mathbb{R}^2)} \leq \eta_0$, then $\Omega(u)$ is empty if and only if $\Omega(v)$ is. If both are empty, then $d_{st}(\mathcal{W}(u),\mathcal{W}(v)) = 0$. Therefore, we are interested only in the case in which both are not empty.

We follow some of the arguments developed in [10, Theorem 4.2], which we briefly sketch for the convenience of the reader.

Let us now assume that u and $v \in \tilde{A}_C$ satisfy $\|u-v\|_{L^1(\mathbb{R}^2)} \leq \eta_0$, and $\Omega(u)$ and $\Omega(v)$ are not empty. For fixed $\varepsilon > 0$, we can find $\eta > 0$ such that if $\|u-v\|_{L^1(\mathbb{R}^2)} \leq \eta$, then $\|\mathcal{I}(u) - \mathcal{I}(v)\|_{L^\infty(B_{\tilde{R}})} \leq \tilde{g}(\varepsilon)$.

Let us now take $x \in \partial\Omega(u)$, that is, $x \in \mathbb{R}^2$ such that $\mathcal{I}(u)(x) = h$. We infer that $|\mathcal{I}(v)(x) - h| \leq \tilde{g}(\varepsilon)$, and therefore by the claim, we deduce that $x \in B_\varepsilon(\partial\Omega(v))$. That is $\partial\Omega(u) \subset B_\varepsilon(\partial\Omega(v))$. By symmetry, we conclude that the Hausdorff distance d_H between $\partial\Omega(u)$ and $\partial\Omega(v)$ is bounded by ε. It has been shown in section 3.3 in [10] that there exist positive constants C_2 and β such that for any $\Omega(u)$ and $\Omega(v)$ belonging to $\mathcal{A}^{1,\alpha}(r, L, R_1)$, we have

$$d_{st}(\Omega(u),\Omega(v)) \leq C_2 \left(d_H(\partial\Omega(u),\partial\Omega(v))\right)^\beta.$$

Therefore, the thesis immediately follows. ∎

We are now in the position to set up our optimization problem. Under the previous definitions and assumptions, let us define the functional $F_0 : A \to [0,+\infty]$ such that

$$F_0(u) = \int |\chi_{\Omega(u)} - \chi_{\Omega_0}| + a|P(\Omega(u)) - P(\Omega_0)| + b\mathcal{P}(u) + c\mathcal{R}(u) \quad \text{for any } u \in A, \tag{3.15}$$

where $\mathcal{P}$ is the functional defined in (2.5), and a, b, and c are positive tuning parameters. We notice that

$$\int |\chi_{\Omega(u)} - \chi_{\Omega_0}| + a|P(\Omega(u)) - P(\Omega_0)| = d_{st}(\mathcal{W}(u), \chi_{\Omega_0}),$$

where d_{st} is the strict convergence distance in $BV(B_{\tilde{R}})$ given in (2.3).

We look for the solution to the following minimization problem:

$$\min\{F_0(u) \,:\, u \in A\}. \tag{3.16}$$

By the direct method, we have that F_0 admits a minimum on A. However, in order to make the minimization problem meaningful, we shall need the following.

3.3. A priori assumptions on minimizers of F_0. We assume that there exists $\tilde{u} \in A$ such that $F_0(\tilde{u})$ is finite and $F_0(\tilde{u}) < |\Omega_0| + aP(\Omega_0)$.

By these assumptions, we exclude the fact that the function $u_0 \equiv 0$ is a minimizer of F_0, and we guarantee that for any minimizer u of F_0, we have that $\Omega(u)$ is not empty. In fact, if $u \in A$ is such that $\Omega(u)$ is empty, we have that

$$F_0(u) \geq F_0(u_0) = |\Omega_0| + aP(\Omega_0) > F_0(\tilde{u}).$$

Let us notice that if instead we replace $\mathcal{R}$ with $\tilde{\mathcal{R}}$ as in Remark 3.4, we just need to assume that there exists $\tilde{u} \in A$ such that $F_0(\tilde{u})$ is finite. In fact, if $u \in A$ is such

that $\Omega(u)$ is empty, we have that $\tilde{\mathcal{R}}(u) = +\infty$ and consequently $F_0(u) = +\infty$. This follows by this simple argument. If $\mathcal{R}(u)$ is finite, then the maximum of $\mathcal{I}(u)$ is either strictly greater than $h+\delta$, and thus $\Omega(u)$ is not empty, or strictly smaller than $h-\delta$, and thus $\tilde{\mathcal{R}}(u) = +\infty$. See the proof of Lemma 3.6.

Moreover, the function $\tilde{u} \in A$ satisfying the previous assumption is the characteristic function of a set of finite perimeter and might be considered a natural choice as an initial guess for any iterative method. We hope that the target set Ω_0 provides such an initial guess; that is, it is desirable that the previous assumption be satisfied by $\tilde{u} = \chi_{\Omega_0}$. As we shall show in the numerical tests, actually in practice it is not always convenient to use as an initial guess the target itself or a small perturbation of it.

We conclude that, under this assumption, if u is a minimizer of F_0, then $u = \chi_E$, where E is a set of finite perimeter and $\Omega(\chi_E)$ is not empty. Such a set E should be chosen as the optimal mask, and $\Omega(\chi_E)$ would be the optimal reconstructed circuit.

The minimization of F_0 presents several challenges from a numerical point of view. Therefore we approximate, in the sense of Γ-convergence, the functional F_0 with a family of functionals $\{F_\varepsilon\}_{\varepsilon>0}$, which are easier to compute with.

We recall that $h > 0$ is the fixed threshold. We take a C^∞ function $\phi : \mathbb{R} \to \mathbb{R}$ such that ϕ is nondecreasing, $\phi(t) = 0$ for any $t \le -1/2$, and $\phi(t) = 1$ for any $t \ge 1/2$. For any $\eta > 0$ let

$$\phi_\eta(t) = \phi\left(\frac{t-h}{\eta}\right) \quad \text{for any } t \in \mathbb{R}.$$

For any $\eta > 0$, let $\Phi_\eta : A \to C^{1,\alpha}(\mathbb{R}^2)$ be defined as

$$\Phi_\eta(u) = \phi_\eta(\mathcal{I}(u)) \quad \text{for any } u \in A. \tag{3.17}$$

Let us summarize the properties of such a function Φ_η.

PROPOSITION 3.8. *For any $\eta > 0$, let $\Phi_\eta : A \to C^{1,\alpha}(\mathbb{R}^2)$ be defined as in* (3.17). *We have that Φ_η is uniformly continuous with respect to the L^1 norm on A and the $C^{1,\alpha}$ norm on $C^{1,\alpha}(B_{\tilde{R}})$.*

Furthermore, for any $C > 0$, Φ_η converges, as $\eta \to 0^+$, uniformly to $\mathcal{W}$ on $\tilde{A}_C$ with respect to the distance d_{st} on $BV(B_{\tilde{R}})$; that is, for any $\varepsilon > 0$ there exists $\eta_0 > 0$ such that, for any η, $0 < \eta \le \eta_0$, we have

$$d_{st}(\Phi_\eta(u), \mathcal{W}(u)) \le \varepsilon \quad \textit{for any } u \in \tilde{A}_C.$$

Proof. The first part is an easy consequence of Proposition 3.1. The second and more important part may be proved analogously to the proof of Proposition 5.1 in [10]. ∎

Furthermore, for any $\gamma > 0$, let us define $\mathcal{R}_\gamma : A \to [0, +\infty]$, satisfying the following properties. First, $\mathcal{R}_\gamma$ is lower semicontinuous, with respect to the L^1 convergence in A. Second, for any $u \in A$ and any $0 < \gamma_1 < \gamma_2$, we have

$$\mathcal{R}_{\gamma_2}(u) \le \mathcal{R}_{\gamma_1}(u) \le \mathcal{R}(u) \quad \text{and} \quad \lim_{\gamma \to 0^+} \mathcal{R}_\gamma(u) = \mathcal{R}(u).$$

Let us denote, for consistency, $\mathcal{R}_0 = \mathcal{R}$.

We shall use the following result.

LEMMA 3.9. *For any $n \in \mathbb{N}$, let $u_n \in A$ and $\gamma_n \ge 0$ be such that, as $n \to \infty$, u_n converges to $u \in A$ in L^1, and γ_n is a nonincreasing sequence converging to* 0. *Then*

we have that

$$\lim_n \mathcal{R}_{\gamma_n}(u_n) = \mathcal{R}(u).$$

Proof. Let us fix $k \in \mathbb{N}$. Then for any $n \geq k$ we have

$$\mathcal{R}_{\gamma_k}(u_n) \leq \mathcal{R}_{\gamma_n}(u_n) \leq \mathcal{R}(u_n).$$

By the semicontinuity of $\mathcal{R}_{\gamma_k}$ and the continuity of $\mathcal{R}$, we infer that for any $k \in \mathbb{N}$,

$$\mathcal{R}_{\gamma_k}(u) \leq \liminf_n \mathcal{R}_{\gamma_k}(u_n) \leq \liminf_n \mathcal{R}_{\gamma_n}(u_n) \leq \limsup_n \mathcal{R}_{\gamma_n}(u_n) \leq \mathcal{R}(u).$$

Letting k go to infinity, we easily conclude the proof. ∎

The main example of such a family of operators $\mathcal{R}_\gamma$ is given by substituting in the definition of $\mathcal{R}$ in (3.13) the function f with a function $f_\gamma : \mathbb{R} \to [0, +\infty]$, that is, to define

$$\mathcal{R}_\gamma(u) = \int_{B_{\bar{R}}} f_\gamma \left(\|\nabla(\mathcal{I}(u))\|^2 - \varphi(\mathcal{I}(u)) \right) \quad \text{for any } u \in A.$$

In order to have the required properties on the family of operators $\mathcal{R}_\gamma$, it is enough that f_γ is continuous on $\mathbb{R}$, and, for any $x \in \mathbb{R}$ and any $0 < \gamma_1 < \gamma_2$, we have

$$f_{\gamma_2}(x) \leq f_{\gamma_1}(x) \leq f(x) \quad \text{and} \quad \lim_{\gamma \to 0^+} f_\gamma(x) = f(x).$$

The main advantage is that in this way we may choose f_γ, which is smooth and real valued everywhere.

We are now in position to describe the approximating functionals and prove the Γ-convergence result. Let us fix a constant p_1, $1 < p_1 < +\infty$, and a continuous function $W : \mathbb{R} \to [0, +\infty)$ such that $W(t) = 0$ if and only if $t \in \{0, 1\}$. Let us denote by $\mathcal{P}_\varepsilon$, $\varepsilon > 0$, the functional defined in (2.4) with $p = p_1$ and the double-well potential W. We recall that the functional $\mathcal{P}$ is defined in (2.5).

Then for any $\varepsilon > 0$, let us define $F_\varepsilon : A \to [0, +\infty]$ such that

$$F_\varepsilon(u) = d_{st}(\Phi_{\eta(\varepsilon)}(u), \chi_{\Omega_0}) + b\mathcal{P}_\varepsilon(u) + c\mathcal{R}_{\gamma(\varepsilon)}(u) \quad \text{for any } u \in A, \tag{3.18}$$

where $\eta : [0, +\infty) \to [0, +\infty)$ is a continuous, increasing function such that $\eta(0) = 0$, and $\gamma : [0, +\infty) \to [0, +\infty)$ is a continuous, nondecreasing function such that $\gamma(0) = 0$. Notice that here we may also assume γ identically equal to zero. Let us observe that, for any $u \in A$,

$$d_{st}(\Phi_{\eta(\varepsilon)}(u), \chi_{\Omega_0}) = \int_{B_{\bar{R}}} |\Phi_{\eta(\varepsilon)}(u) - \chi_{\Omega_0}| + a \left| \int_{B_{\bar{R}}} \|\nabla(\Phi_{\eta(\varepsilon)}(u))\| - P(\Omega_0) \right|.$$

By the direct method, each of the functionals F_ε, $\varepsilon > 0$, admits a minimum over A. We now state the Γ-convergence result.

THEOREM 3.10. *As $\varepsilon \to 0^+$, F_ε Γ-converges to F_0 on A with respect to the L^1 norm.*

Proof. Let us fix $\varepsilon_n > 0$, $n \in \mathbb{N}$, such that ε_n converges to 0 as $n \to \infty$. Let $F_n = F_{\varepsilon_n}$ and let $u \in A$. Without loss of generality, we may assume that ε_n is decreasing with respect to $n \in \mathbb{N}$.

We begin with the Γ-lim inf inequality. Let $u_n \in A$, $n \in \mathbb{N}$, be such that u_n converges to u in L^1. Without loss of generality, we may assume that $F_n(u_n)$, $n \in \mathbb{N}$, is uniformly bounded by a constant C. Then by Lemma 3.9, and by the continuity of $\mathcal{R}$, we infer that u and u_n, for any $n \in \mathbb{N}$ large enough, belong to $\tilde{A}_C$. Then

$$d_{st}(\Phi_{\eta(\varepsilon_n)}(u_n), \mathcal{W}(u)) \leq d_{st}(\Phi_{\eta(\varepsilon_n)}(u_n), \mathcal{W}(u_n)) + d_{st}(\mathcal{W}(u_n), \mathcal{W}(u)).$$

As $n \to \infty$, the first term on the right-hand side converges to 0 by Proposition 3.8, whereas the second converges to 0 by Lemma 3.7. Therefore, the Γ-lim inf inequality immediately follows by the Γ-convergence of $\mathcal{P}_\varepsilon$ to $\mathcal{P}$ and Lemma 3.9.

Concerning the recovery sequence, without loss of generality we may restrict ourselves to the case in which $F_0(u)$ is finite. The Γ-convergence of $\mathcal{P}_\varepsilon$ to $\mathcal{P}$ allows us to find $u_n \in A$, $n \in \mathbb{N}$, such that u_n converges to u in L^1 and $\mathcal{P}_{\varepsilon_n}(u_n)$ converges to $\mathcal{P}(u)$. By Lemma 3.9 and reasoning analogous to that developed for the Γ-lim inf inequality, we immediately conclude that $F_n(u_n)$ converges to $F_0(u)$. ∎

PROPOSITION 3.11. *There exist $\tilde{\varepsilon} > 0$ and a compact subset $\mathcal{K}$ of A such that for any ε, $0 < \varepsilon \leq \tilde{\varepsilon}$, we have*

$$\min_{\mathcal{K}} F_\varepsilon = \min_{A} F_\varepsilon.$$

Proof. By the Γ-convergence result, in particular by the construction of the recovery sequence applied to a minimizer of F_0, we infer that there exist $\tilde{\varepsilon} > 0$ and a positive constant C_1 such that for any ε, $0 < \varepsilon \leq \tilde{\varepsilon}$, we have $\inf_A F_\varepsilon = \min_A F_\varepsilon \leq C_1$. Let $u_\varepsilon \in A$, $0 < \varepsilon \leq \tilde{\varepsilon}$, be such that $F_\varepsilon(u_\varepsilon) = \min_A F_\varepsilon$. Then we observe that the set $\{u_\varepsilon\}_{0<\varepsilon\leq\tilde{\varepsilon}}$ satisfies the properties of Proposition 2.3 for some constant C. Therefore, $\{u_\varepsilon\}_{0<\varepsilon\leq\tilde{\varepsilon}}$ is precompact in $L^1(\mathbb{R}^2)$, and the proof is concluded. ∎

Using Theorem 3.10 and Proposition 3.11, we apply the fundamental theorem of Γ-convergence to conclude with the following result.

THEOREM 3.12. *We have that F_0 admits a minimum over A and*

$$\min_A F_0 = \lim_{\varepsilon\to 0^+} \inf_A F_\varepsilon = \lim_{\varepsilon\to 0^+} \min_A F_\varepsilon.$$

Let ε_n, $n \in \mathbb{N}$, be a sequence of positive numbers converging to 0. For any $n \in \mathbb{N}$, let $F_n = F_{\varepsilon_n}$. If $\{u_n\}_{n=1}^\infty$ is a sequence contained in A which converges, as $n \to \infty$, to $u \in A$ in L^1 and satisfies $\lim_n F_n(u_n) = \lim_n \inf_A F_n$, then u is a minimizer of F_0 on A; that is, u solves the minimization problem (3.16).

We notice that if $\{u_n\}_{n=1}^\infty$ is a sequence contained in A such that $\lim_n F_n(u_n) = \lim_n \inf_A F_n$, then, again by Proposition 2.3, we have that, up to a subsequence, u_n converges, as $n \to \infty$, to a function $u \in A$ in L^1, where u is a minimizer of F_0 on A.

Finally, we point out the following remark that may be of use in the numerical computation of the minimizers.

Remark 3.13. All of the results remain valid also with the following modifications. Since we are dealing only with $BV(B_{\tilde{R}})$ functions, whose values are between 0 and 1, we may replace, in the definition of F_0 and F_ε, $\varepsilon > 0$, the distance d_{st} with the distance-like function d_{st}^p, for any p, $1 \leq p < +\infty$, defined as follows:

$$d_{st}^p(u, v) = \int_{B_{\tilde{R}}} |u - v|^p + a\big||Du|(B_{\tilde{R}}) - |Dv|(B_{\tilde{R}})\big| \quad \text{for any } u,\, v \in BV(B_{\tilde{R}}, [0, 1]).$$

Moreover, we may allow in all cases the parameter a to be equal to 0.

4. The numerical experiments. For some positive ε we shall minimize the functional F_ε defined in (3.18), with d_{st} replaced by d_{st}^2 (see Remark 3.13) and where the tuning parameter a is allowed to be 0.

Let Ω be the computational domain that for simplicity we choose as a square centered in the origin. We assume that u is always a real valued function on Ω and is extended to zero outside Ω.

Following [12], we use the kernel K defined in (3.2) and approximate the mutual intensity function J defined in (3.3) and (3.4) by

$$J_{approx}(x) = \int_{\mathbb{R}^2} \frac{1}{\pi(k\sigma \mathrm{NA})^2} \mathrm{e}^{-\beta|\xi|^2} \mathrm{e}^{\mathrm{i}\xi\cdot x} \mathrm{d}\xi, \quad x \in \mathbb{R}^2,$$

where

$$\beta = \frac{\log 2}{(k\sigma \mathrm{NA})^2}.$$

Correspondingly, the intensity function can be approximated as follows:

$$\mathcal{I}_{approx}(u)(x) = \int_{\mathbb{R}^2}\int_{\mathbb{R}^2} u(x-\xi)H(\xi,\eta)u(x-\eta)\mathrm{d}\xi\mathrm{d}\eta, \quad x \in \mathbb{R}^2,$$

where

$$H(\xi,\eta) = K(\xi)J_{approx}(\eta-\xi)\overline{K}(\eta).$$

Here H is the Hopkins transmission cross coefficients (TCC) function. The advantage of using the Hopkins model is that the TCC function is independent of the mask function m; therefore, given an optical system, the TCC function need only be computed once.

In the discrete formulation, we subdivide Ω into $N \times N$ squares with sides of length $\Delta x = \Delta y$. Setting $i = (i_1, i_2)$, $j = (j_1, j_2)$, and $k = (k_1, k_2)$, with i, j, $k \in \{1, \dots, N\} \times \{1, \dots, N\}$, we have

$$\mathcal{I}_{discr}(u)(i) = \sum_k \sum_j \left(u(i-k)H(k,j)u(i-j)\right) \Delta x^2 \Delta y^2,$$

where u is an $N \times N$ real valued matrix, whereas H is here an $N^2 \times N^2$ matrix. We notice that for any $N \times N$ matrix M, we shall always assume that $M(i) = 0$ for any $i \in \mathbb{Z}^2$ such that $i \notin \{1, \dots, N\} \times \{1, \dots, N\}$. Analogously we are assuming that $H(k,j) = 0$ for any $(k,j) \in \mathbb{Z}^2 \times \mathbb{Z}^2$ such that either $k \notin \{1, \dots, N\} \times \{1, \dots, N\}$ or $j \notin \{1, \dots, N\} \times \{1, \dots, N\}$; that is, we are introducing here another approximation since we are dropping H to zero outside $\Omega \times \Omega$.

Following the arguments in [12], we notice that H is a positive, semidefinite Hermitian matrix, and we decompose H through a singular value decomposition, actually through the following eigenfunction expansion:

$$H(k,j) = \sum_n \sigma_n V_n(k)\overline{V_n}(j),$$

where σ_n are the nonnegative eigenvalues, which we assume to be decreasing with respect to n, and V_n are the corresponding eigenfunctions. In general, due to the fast

decay of its eigenvalues, we can approximate H by its dominant eigenvectors; that is, we may further approximate our intensity functional by using, instead of H,

$$H_{trunc}(k,j) = \sum_{n=1}^{N_0} \sigma_n V_n(k)\overline{V_n}(j)$$

for a suitably low number N_0. This leads to further improvement on the computational efficiency of the aerial intensity. Moreover, similar to the TCC function, the eigenvalues and eigenvectors are precomputable when the optical system is fixed. Since N_0 is usually small, using H_{trunc} instead of H decreases the computational cost of repeated intensive calculations in the inverse problem.

Finally, instead of $\mathcal{I}$, we use the discrete approximated functional I defined as follows:

$$\frac{I(u)(i)}{\Delta x^2 \Delta y^2} = \sum_{n=1}^{N_0} \sigma_n \sum_{k,j} \left(u(i-k)V_n(k)\overline{V_n}(j)u(i-j)\right) = \sum_{n=1}^{N_0} \sigma_n (V_n * u)(i)\overline{(V_n * u)}(i)$$

for any real valued $N \times N$ matrix u. We notice that $*$ denotes the discrete convolution of matrices, and we recall that any $N \times N$ matrix is extended to zero on any index $i \in \mathbb{Z}^2$ such that $i \notin \{1,\dots,N\} \times \{1,\dots,N\}$.

For our numerical computations, we shall use a very simple approach, namely a gradient method. We recall that our functionals are nonconvex, and therefore local instead of global minimizers might be obtained.

In order to use a gradient method for our numerical computations we need to compute differentials with respect to u of functionals applied to $I(u)$. For simplicity, for the time being we set $\Delta x = \Delta y = 1$. Given u, a real valued $N \times N$ matrix, and the variation v, another real valued $N \times N$ matrix, we have that

$$DI(u)[v] = 2\Re\left(\sum_{n=1}^{N_0} \sigma_n (V_n * u)\overline{(V_n * v)}\right).$$

Let us begin with the following simpler case. Let $F(u) = \int f(I(u)) = \sum_k f(I(u)(k)) \in \mathbb{R}$ for some real valued function f. We need to compute $\nabla_u F(u) \in \mathbb{R}^{N\times N}$. We remark that, if e_{i_1,i_2} is the matrix which is one in (i_1,i_2) and zero elsewhere, then $\nabla_u F(u)(i_1,i_2) = DF(u)[e_{i_1,i_2}]$. Using the same argument as before, we obtain

$$DF(u)[e_{i_1,i_2}] = 2\Re\left(\sum_{n=1}^{N_0} \sigma_n \left(\sum_k f'(I(u))(k)(V_n * u)(k)\overline{(V_n * e_{i_1,i_2})}(k)\right)\right).$$

But $(V_n * e_{i_1,i_2})(k) = V_n(k-i)$, with $i = (i_1,i_2)$. Let us call $W_n(\cdot) = \overline{V_n(-\cdot)}$. Then summing on k we have

$$\sum_k f'(I(u))(k)(V_n * u)(k)\overline{(V_n * e_{i_1,i_2})}(k)$$
$$= \sum_k f'(I(u))(k)(V_n * u)(k)W_n(i-k) = \left(W_n * \left(f'(I(u))(V_n * u)\right)\right)(i).$$

In conclusion,

$$\nabla_u F(u) = 2\Re\left(\sum_{n=1}^{N_0} \sigma_n \left(W_n * \left(f'(I(u))(V_n * u)\right)\right)\right).$$

Let us notice that, assuming our computational domain is centered in 0, we can easily compute W_n through the MATLAB command $W_n = \texttt{conj}(\texttt{flipud}(\texttt{fliplr}(V_n)))$.

Now let

$$\tilde{F}(u) = \int \tilde{f}(\nabla f(I(u))) = \sum_k \tilde{f}\left(\partial_{x_1}(f(I(u)))(k), \partial_{x_2}(f(I(u)))(k)\right) \in \mathbb{R},$$

where $\tilde{f}$ is a real valued function defined on $\mathbb{R}^2$, and ∂_{x_l}, $l = 1, 2$, are partial derivatives with respect to the two variables, in any finite differences sense. Again we need to compute $\nabla_u \tilde{F}(u) \in \mathbb{R}^{N\times N}$. We denote by $\tilde{f}_1$ the partial derivative of $\tilde{f}$ with respect to the first variable and by $\tilde{f}_2$ the partial derivative of $\tilde{f}$ with respect to the second variable. Then similarly we have

$$\nabla_u \tilde{F}(u) = 2\Re\left(\sum_{n=1}^{N_0} \sigma_n\left(W_n * A + ((Z_n)_1 * \overline{B_1}) + ((Z_n)_2 * \overline{B_2})\right)\right),$$

where $W_n(\cdot) = \overline{V_n(-\cdot)}$, $(Z_n)_1(\cdot) = (\partial_{x_1} V_n)(-\cdot)$, $(Z_n)_2(\cdot) = (\partial_{x_2} V_n)(-\cdot)$, and

$$A = \sum_{l=1}^{2}\left(\tilde{f}_l(\nabla f(I(u)))\partial_{x_l}(f'(I(u)))(V_n * u) + \tilde{f}_l(\nabla f(I(u)))f'(I(u))(\partial_{x_l} V_n * u)\right),$$

$$B_1 = \tilde{f}_1(\nabla f(I(u)))f'(I(u))(V_n * u), \quad B_2 = \tilde{f}_2(\nabla f(I(u)))f'(I(u))(V_n * u).$$

Let us now investigate $\partial_{x_1} I(u)$. We have that

$$\partial_{x_1} I(u) = 2\Re\left(\sum_{n=1}^{N_0} \sigma_n(\partial_{x_1} V_n * u)\overline{(V_n * u)}\right).$$

Therefore,

$$D(\partial_{x_1} I(u))[v] = 2\Re\left(\sum_{n=1}^{N_0} \sigma_n\left[(\partial_{x_1} V_n * u)\overline{(V_n * v)} + (\partial_{x_1} V_n * v)\overline{(V_n * u)}\right]\right).$$

Finally, for a real valued function g defined on $\mathbb{R}^2$, let

$$G(u) = \int g(\|\nabla_{x_1,x_2} I(u)\|^2, I(u)) = \sum_k g\left(\|\nabla_{x_1,x_2} I(u)\|^2(k), I(u)(k)\right) \in \mathbb{R}.$$

We denote by g_1 the partial derivative of g with respect to the first variable and by g_2 the partial derivative of g with respect to the second variable. A completely similar computation leads to

$$\nabla_u G(u) = 2\Re\left(\sum_n \sigma_n(A_1 + A_2 + \tilde{B}_1 + \tilde{B}_2 + C)\right),$$

where, for $l = 1, 2$,

$$A_l = W_n * (2g_1(\|\nabla_{x_1,x_2} I(u)\|^2, I(u))\partial_{x_l} I(u)(\partial_{x_l} V_n * u)),$$

$$\tilde{B}_l = (Z_n)_l * (2g_1(\|\nabla_{x_1,x_2} I(u)\|^2, I(u))\partial_{x_l} I(u)\overline{(V_n * u)}),$$

$$C = W_n * (g_2(\|\nabla_{x_1,x_2} I(u)\|^2, I(u))(V_n * u)).$$

With these results we can compute the gradient for any term of our functional to be minimized. For example, the discretized version of our regularization functional $\mathcal{R}_\gamma$ may be expressed as

$$\mathcal{R}_\gamma(u) = \int f_\gamma\left(\|\nabla_{x_1,x_2} I(u)\|^2 - \varphi(I(u))\right),$$

that is, $f_\gamma(\|\nabla_{x_1,x_2} I(u)\|^2 - \varphi(I(u))) = g(\|\nabla_{x_1,x_2} I(u)\|^2, I(u))$, where $g(a,b) = f_\gamma(a - \varphi(b))$, and hence $g_1(a,b) = f'_\gamma(a-\varphi(b))$ and $g_2(a,b) = -f'_\gamma(a-\varphi(b))\varphi'(b)$.

In our numerical experiments we shall use the following common parameters. The computational domain is $1600nm \times 1600nm$ and, since we take $N = 128$, is subdivided into 128×128 squares, each with sides of length $\Delta x = \Delta y = 12.5nm$.

We use the first $N_0 = 10$ eigenvalues in H_{trunc} and consider the optical system with the following physical parameters:

$$\lambda = 2\pi/k = 193nm, \quad NA = 1, \quad \sigma = 0.067.$$

These correspond to the parameters used in [12] even if our notation is slightly different. Actually, in the numerical computation we use the eigenvalues σ_n and eigenfunctions V_n computed in [12].

About the perimeter approximation $\mathcal{P}_\varepsilon$ defined in (2.4) we choose $p = 2$ and $W(s) = s(1-s)$ for any $0 \le s \le 1$. Since in our computation we are dropping in $\mathcal{P}_\varepsilon$ the constant c_p, in this section the parameter b actually corresponds to b/c_p in the notation of the previous section.

We choose f_γ to be an approximation from below of f, where f is defined as in (3.11) with $\alpha = 1$, and φ is as in (3.12). Normalizing the threshold h to be equal to 1 and the length of the pixel $\Delta x = \Delta y$ to be equal to 1 as well, the term $\mathcal{R}_\gamma$ penalizes critical values of the intensity $I(u)$ close to 1; namely, the worst situation is when the triple $(I(u), \partial_{x_1} I(u), \partial_{x_2} I(u))$ is equal to $(1,0,0)$. If we call d the distance between $(I(u), \partial_{x_1} I(u), \partial_{x_2} I(u))$ and $(1,0,0)$, in the Euclidean norm, that is,

(4.1)
$$d = \sqrt{(I(u)-1)^2 + (\partial_{x_1} I(u))^2 + (\partial_{x_2} I(u))^2} \quad \text{(normalized } h = 1, \Delta x = \Delta y = 1),$$

the aim of $\mathcal{R}_\gamma$ is not to let d go to zero at any point; actually we wish to avoid the case in which d, in this normalized setting, is of the order of 5% or less. Therefore, we choose $\mathcal{R}_\gamma$ in such a way that it strongly penalizes the case in which d is less than or equal to 5% and has no effect whatsoever when d is above 7%. We keep this property fixed for any γ and let the values of f_γ, and thus the value of $\mathcal{R}_\gamma$, increase as the positive parameter γ goes to 0.

We start with an initial value of ε, η, and γ, namely $\varepsilon_0 = 0.002$, $\eta_0 = 0.2$, and $\gamma_0 = 0.03$, and its corresponding functional F_{ε_0}, and a suitable initial guess $u_{initial}$. By a gradient method, namely a standard steepest descent, we look for u_0, a minimizer of F_{ε_0}, using 60 iterations. Then we update the parameters ε, η, and γ by dividing their previous values by the corresponding decrease rate given by $rate_\varepsilon$, $rate_\eta$, and $rate_\gamma$, respectively. We use the computed minimizer u_0 of F_{ε_0} as the initial guess and minimize the functional F_ε with the updated parameters. We repeat the procedure after any 60 iterations. The aim of such a procedure is the following. We wish to start with relatively large values of the parameters ε, η, and γ that allow a rather fast evolution of the phase-field variable u. Therefore, we have a fast convergence to a reasonably good mask, no matter what the initial guess. Such a mask provides us with a good initial guess for the next functional, with lower values of the parameters,

that allows us to refine such a mask. After we have decreased the parameters a fixed number of times, we consider the computed minimizer of the last final functional F_ε as our final optimal phase-field function u. The final optimal mask is obtained from this numerical solution of the phase-field variable u by taking the set where $u > 1/2$. With this iterative procedure of updating the parameters, we then obtain a minimizer of our last functional starting from a rather good initial guess. This is important since, for extremely small values of our parameters, the evolution of u is extremely slow, and therefore we need to start rather close to the sought-after minimizer. We also notice that, during this procedure, the parameters become rather small. Therefore, as we shall show in our tests, due to the presence of the Modica–Mortola functional, on most occasions the final optimal phase-field function u is already binary, taking values 0 and 1 only, and therefore it coincides with the final optimal mask. If this does not happen, then u is different from 0 and 1 only in very few pixels, and the value of u on these pixels keeps oscillating from iteration to iteration. We conjecture that this may be due to the fact that we struck a local minima in the process. We finally notice that the numerical experiments show that in general it is better to keep these decrease rates rather close to 1.

We recall that, given a phase-field function u, which is a function on the computational domain with values in $[0, 1]$, its outcome pattern is the region where the light intensity is over the threshold value h. The threshold in our tests equals 40% of the maximum value of I_0, where I_0 is the intensity when the mask is exactly the target pattern, that is, $h = 40 \max(I_0)/100$.

We now describe the outcome of our numerical tests. We shall use two different types of targets, shown in Figure 1. The first target pattern, Target 1, is composed of two features. The smallest width of the outside feature is 10 pixels, the width of the inside vertical bar is 13 pixels, and two features are at least 12 pixels apart from each other. The second target pattern, Target 2, is more complicated and consists of four features, with width as small as 8 pixels and distance between two different features as small as 6 pixels.

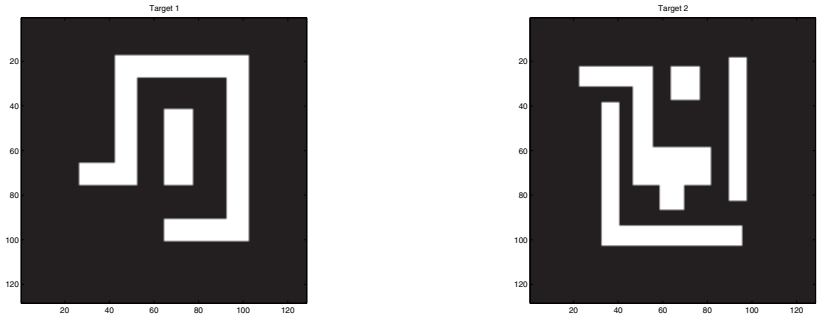

FIG. 1. *Test target patterns. Left: Target* 1. *Right: Target* 2.

First, we briefly discuss tests regarding Target 1, then we move to the more interesting Target 2.

Target 1. In these tests we use the following parameters. The weight of the term containing the difference between the two perimeters or, more precisely, the two total variations, in the distance function d_{st}^2 is $a = 0$; the weight of the Modica–Mortola term $\mathcal{P}_\epsilon$ is $b = 2 \times 10^{-4}$. The weight of the regularization term $\mathcal{R}_\gamma$ is $c = 0$. Moreover, we set $rate_\varepsilon = 1.2$, $rate_\eta = 1.2$, and $rate_\gamma = 1.05$ and perform 1080

iterations in total; that is, we decrease our parameters 17 times. Correspondingly, at the end we compute the minimizer of the final functional F_ε corresponding to the parameters $\varepsilon = \varepsilon_0 \times rate_\varepsilon^{-17} \approx 9 \times 10^{-5}$, $\eta = \eta_0 \times rate_\eta^{-17} \approx 9 \times 10^{-3}$, and $\gamma = \gamma_0 \times rate_\gamma^{-17} \approx 1.3 \times 10^{-2}$.

We use two different initial guesses. In *Test n.*1 we consider an initial guess which is a smooth perturbation of the target itself, and in *Test n.*2 the initial guess is much more diffuse and has nothing to do with the target itself. The results are presented in Figure 2. Let us notice that for initial guesses and masks, the value 0 is depicted in black, whereas the value 1 is in white. Concerning the output, we show the difference between the exposed pattern and the target. Namely, in white we have the part of the exposed pattern which is outside the target and in black the part of the target that is not contained in the exposed pattern. The black line is the profile of the target.

First, we have that in both cases we converge to a binary function, due to the effect of the Modica–Mortola functional. The mask so obtained is very diffuse, even with an initial guess which is not. Actually, the reconstruction is better when the initial guess is more diffuse. In fact the difference between the exposed pattern and the target pattern is 61 pixels in *Test n.*1 and 44 pixels in *Test n.*2, and the output is also visibly better. We also notice that the two masks are rather different in shape; this may be due to the fact that the original functional F_0 may have several local minima and different initial guesses, or different choices of the parameters, may therefore lead to quite different masks.

Since, in both cases, the intensity corresponding to the phase-fields during the iterations has never reached a critical point with value near the threshold, the result does not change even if we add the regularization term $\mathcal{R}_\gamma$ (we have tested it with its coefficient c varying from 5×10^{-4} to 2×10^{-3}) in accordance with the theory.

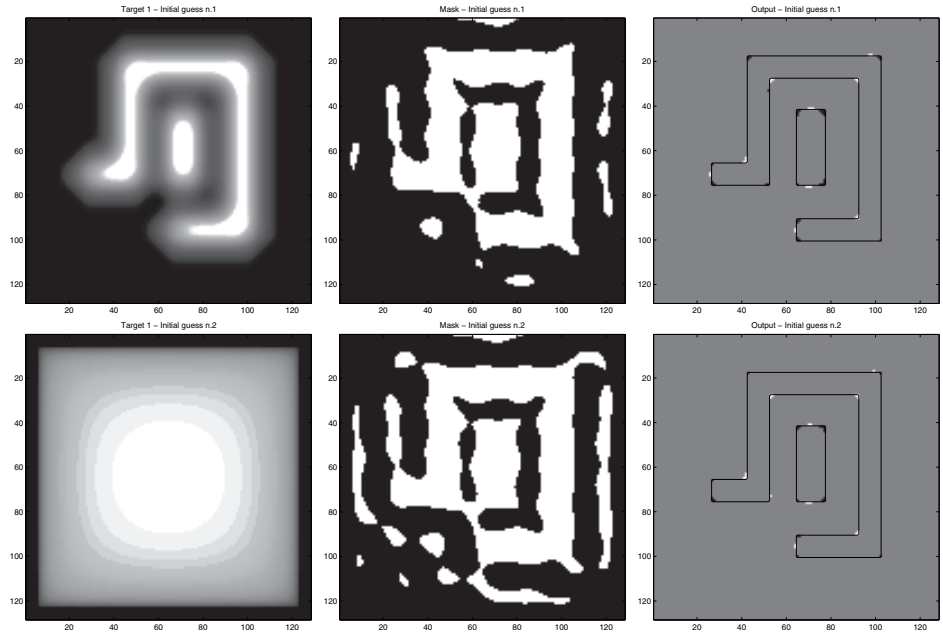

FIG. 2. *Top: Test n.*1. *Left: initial guess n.*1. *Middle: mask. Right: output. Bottom: Test n.*2. *Left: initial guess n.*2. *Middle: mask. Right: output.*

In order to verify that having a diffuse mask with a lot of assist features is an advantage, we took the initial guess of *Test n.*1, but we impose that our phase-fields during our iterations (and consequently our final mask) be kept to zero outside a fixed neighborhood of the target. The outcome is worse, with the difference in pixels from the target being 66. See Figure 3.

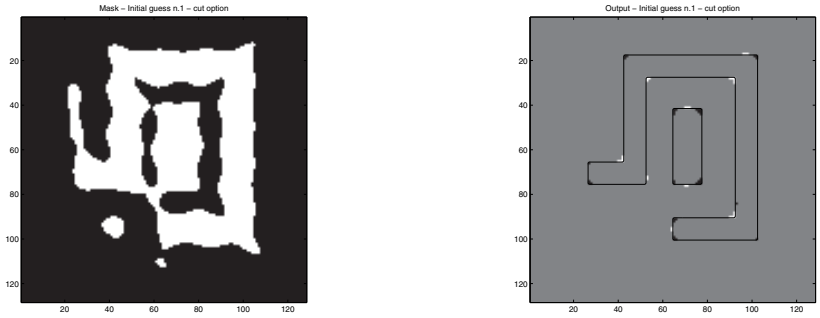

FIG. 3. *Test n.*3 *(cut option). Left: mask. Right: output.*

Target 2. In the first two tests we use the same parameters as for Target 1, namely the weight of the difference between the perimeters in the distance function is $a = 0$; the weight of the Modica–Mortola term $\mathcal{P}_\epsilon$ is $b = 2 \times 10^{-4}$. The weight of the regularization term $\mathcal{R}_\gamma$ is $c = 0$. Moreover, we set $rate_\varepsilon = 1.2$, $rate_\eta = 1.2$, and $rate_\gamma = 1.05$ and perform 1080 iterations in total.

We first investigate two tests with different initial guesses. In *Test n.*1 we consider an initial guess which is a smooth perturbation of the target itself. In *Test n.*2 the initial guess is much more diffuse and has nothing to do with the target; it is actually the same as in *Test n.*2 for Target 1. The results are presented in Figure 4, and the conclusions are similar to those discussed for Target 1. Notice that the difference between exposed pattern and target is 233 for *Test n.*1 and 227 for *Test n.*2. Hence, we use the diffuse initial guess of *Test n.*2 in all of the following tests.

We shall discuss in detail the effect of the regularization term R_γ, the main theoretical novelty of the paper. Since it penalizes critical points at values close to the threshold value h, its effect should be the one to make the reconstruction more stable with respect to perturbations of h, especially from a topological point of view.

We consider the following two cases. In the first case we keep the parameters of *Test n.*2 except the value of the coefficient c of $\mathcal{R}_\gamma$. Namely, *Test n.*3 is exactly the same as *Test n.*2 ($c = 0$), whereas for *Test n.*4 we set $c = 5 \times 10^{-4}$, and for *Test n.*5 we set $c = 2 \times 10^{-3}$; that is, we steadily increase the coefficient of $\mathcal{R}_\gamma$.

Notice that here sometimes the final optimal phase-field function u is not binary; however, the number of pixels where u is different from 0 and 1 is very limited. As already mentioned, when this happens we are most likely stuck near a local minimum of the final functional F_ε.

We remark that there seems to be not much difference in the masks (which are not shown) and the outputs (the error in pixels is 227 for *Test n.*3, 225 for *Test n.*4, and 227 again for *Test n.*5). However, $\mathcal{R}_\gamma$ prevents the threshold from being a critical value. In fact, the minimal value of the function d defined above in (4.1) goes from 1.27% in *Test n.*3 to 2.24% in *Test n.*4 and finally to 4.35% in *Test n.*5. The benefit of the penalty is stability with respect to the changes of the threshold h, as we shall shortly see. We change the value of the threshold by a percentage value of *hvar*. The

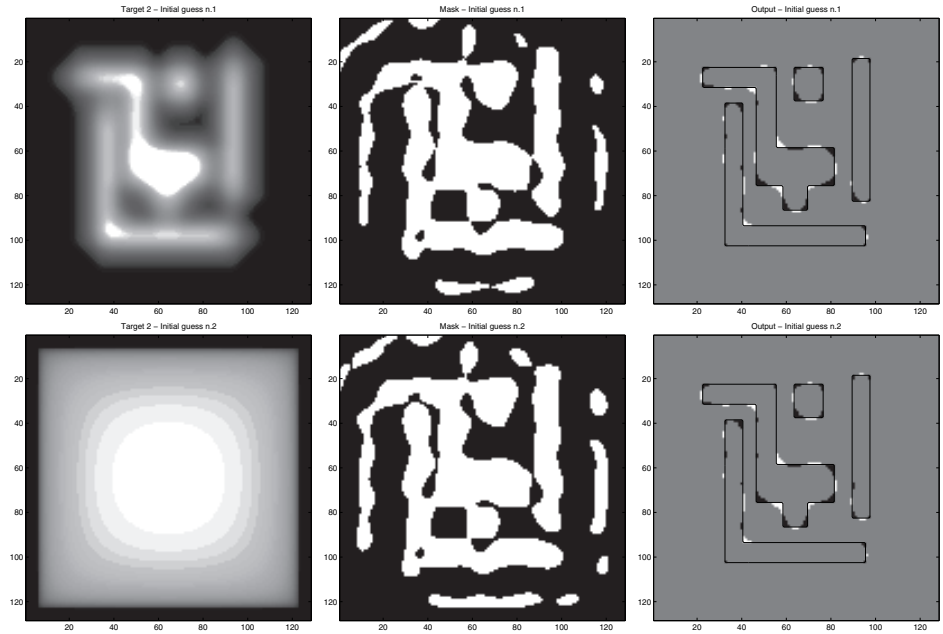

FIG. 4. *Top: Test n.*1. *Left: initial guess n.*1. *Middle: mask. Right: output. Bottom: Test n.*2. *Left: initial guess n.*2. *Middle: mask. Right: output.*

outcome is shown in Figure 5. On the top we have *Test n.*3 (with $c = 0$), in the middle we have *Test n.*4 ($c = 5 \times 10^{-4}$), and on the bottom we have *Test n.*5 ($c = 2 \times 10^{-3}$). From left to right we see how the reconstruction changes if we vary the value of the threshold. On the left the threshold is h (corresponding to $hvar = 0$), in the middle it is $(100.5/100)h$ ($hvar = 0.5$), and on the right it is $(102.5/100)h$ ($hvar = 2.5$). Even if the improvement by increasing the parameter c is not that striking from the point of view of the error in pixels, from a topological point of view it is actually remarkable. In fact, when $c = 0$, a hole appears in the reconstruction in the middle of the bigger feature of the target if we just slightly perturb the threshold of 0.5%. On the contrary, such a hole appears at a much higher quote as c increases.

This is even more striking in another example where we decrease ε, η, and γ faster by using $rate_\varepsilon = 1.5$, $rate_\eta = 1.5$, and $rate_\gamma = 1.1$, and we perform 780 iterations in total. Keeping all of the other parameters fixed, we call *Test n.*6 the one with $c = 0$, *Test n.*7 the one with $c = 5 \times 10^{-4}$, and, finally, *Test n.*8 the one with $c = 2 \times 10^{-3}$. The outcome is shown in Figure 6. On the top we have *Test n.*6 (with $c = 0$), in the middle we have *Test n.*7 ($c = 5 \times 10^{-4}$), and on the bottom we have *Test n.*8 ($c = 2 \times 10^{-3}$). From left to right we see how the reconstruction changes if we vary the value of the threshold. On the left the threshold is $(99.5/100)h$ ($hvar = -0.5$), in the middle it is h ($hvar = 0$), and on the right it is $(103.5/100)h$ ($hvar = 3.5$).

In *Test n.*6, without the regularization term $\mathcal{R}_\gamma$, the hole appears even if we take a threshold lower than h. The hole is not present for threshold h if we add $\mathcal{R}_\gamma$ with a small coefficient, and it is not present for a considerably higher value of the threshold (+3.5%) if the coefficient of $\mathcal{R}_\gamma$ is slightly bigger.

So far we have kept the coefficient a equal to 0. In fact, in our experiments we see that the term containing the difference between the perimeters in the definition of the distance function d_{st}^2 actually does not play a big role and in general does not

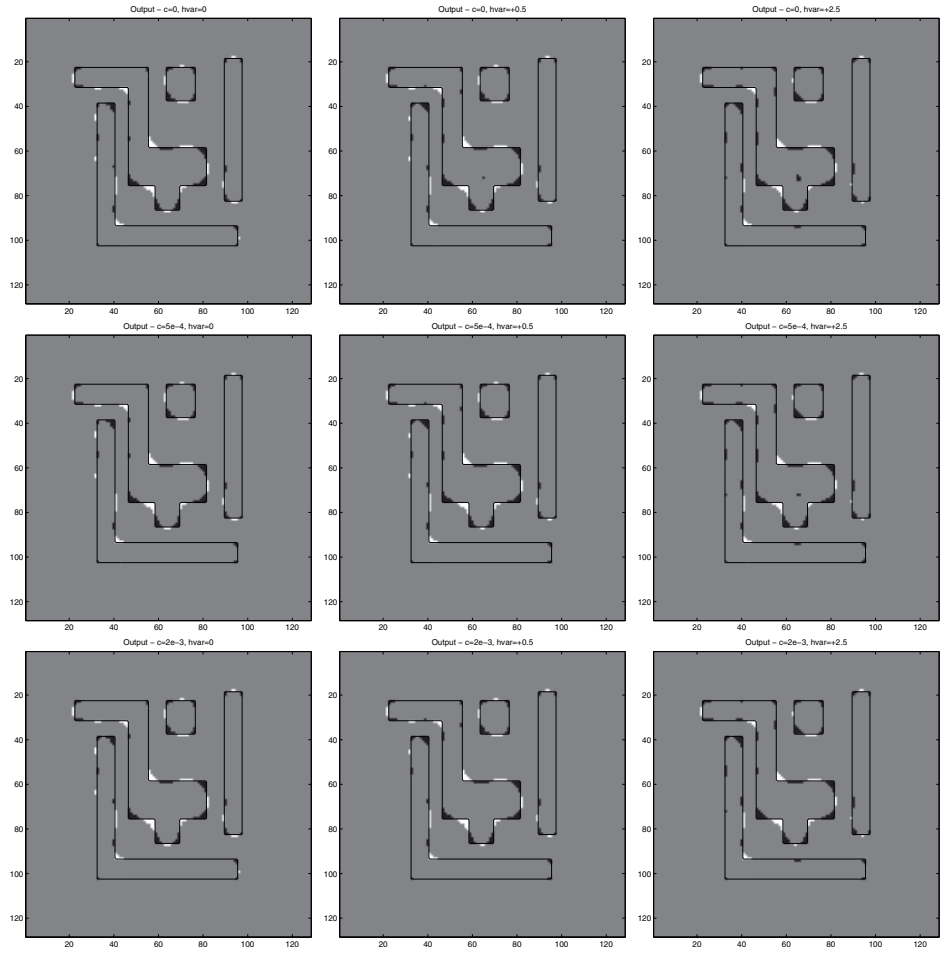

FIG. 5. *Top: Test n.*3 *($c = 0$). Middle: Test n.*4 *($c = 5 \times 10^{-4}$). Bottom: Test n.*5 *($c = 2 \times 10^{-3}$). Left: $hvar = 0$. Middle: $hvar = 0.5$. Right: $hvar = 2.5$.*

improve the reconstruction. As pointed out earlier, this is due to the smoothing effect of the operator I that does not make very relevant the smoothing effect provided by the difference between the two perimeters. Moreover, the difference between the two perimeters is just the difference between two numbers, and therefore this term is absolutely nonlocal. It might be interesting to develop a new distance that takes into account the difference between the two perimeters not only globally but also locally. This could also help to sharpen corners as much as possible. However, the construction of such a new distance is beyond the scope of this paper. For completeness we show the outcome of an experiment where the full functional is used; namely, we modify *Test n.*4 above by changing the parameter a from 0 to 0.5. The error in pixels is 232 in this case, and the outcome is illustrated in Figure 7.

5. Conclusions. From our numerical experiments we can draw the following general conclusions.

1. The outcome mask is very diffuse and is not at all close to target. While the optimal mask has shapes much more complicated than the target, the

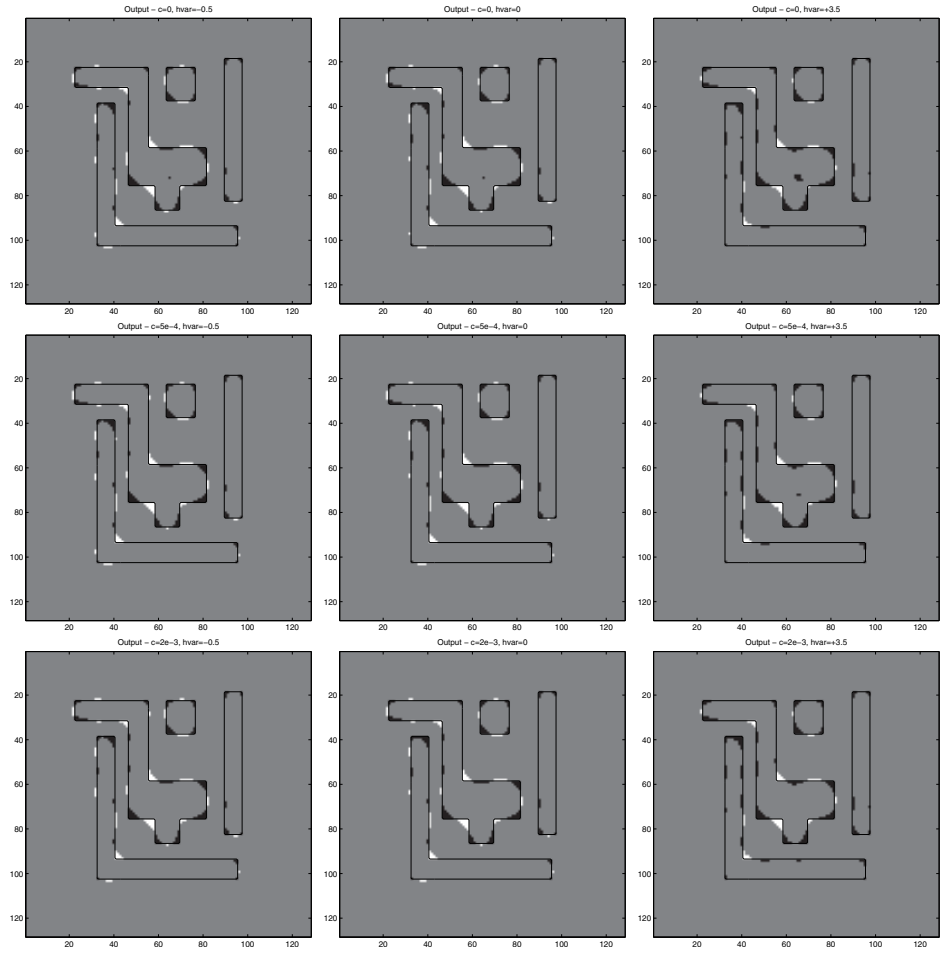

FIG. 6. *Top: Test n.*6 *($c = 0$). Middle: Test n.*7 *($c = 5 \times 10^{-4}$). Bottom: Test n.*8 *($c = 2 \times 10^{-3}$). Left: $hvar = -0.5$. Middle: $hvar = 0$. Right: $hvar = 3.5$.*

exposed region is close to the target. The main reason for these two facts is the high nonlocality of the image intensity.

2. The final shape of the mask strongly depends on the initial guess, since the functional F_0 is nonconvex and therefore may have several absolute and local minimizers.
3. The presence of several local minima, in this case of the approximated functional F_ε, also has the effect that sometimes we do not have convergence to a perfectly binary function. However, the discrepancy with a binary function is limited to very few pixels.
4. We observed that the reconstruction is, in general, better when the parameters decrease slowly and uniformly.
5. The effect of the term containing the difference between the two perimeters in the definition of the distance d_{st}^2 does not have a pronounced influence on the optimal mask.

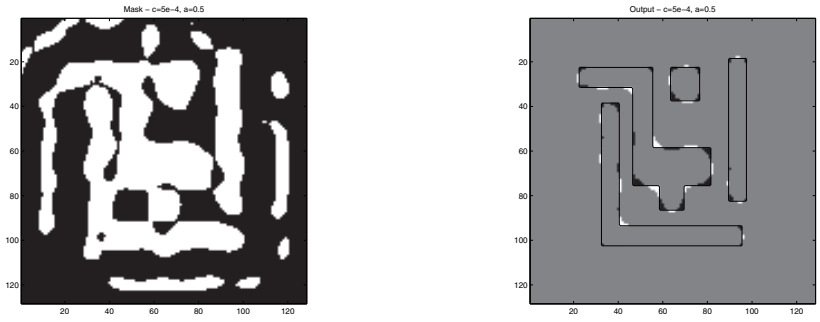

FIG. 7. *Test n.9 ($c = 5 \times 10^{-4}$, $a = 0.5$). Left: mask. Right: output.*

6. Discussion. In this paper we studied the inverse problem of photolithography, which can be viewed as an optimal shape design problem. A main novelty of the paper is the regularization term $\mathcal{R}$, which has both theoretical and practical value. In solving the inverse problem, the penalty term has a desirable stabilizing influence.

When the threshold h is not close to a critical value of the intensity, the penalty term has no effect. This is what happens when we perform the computation using Target 1. For Target 2, the intensity has a local minimum inside the biggest feature with a local minimum value very close to the threshold. This is why a hole may appear in the reconstruction for small perturbations of the threshold. In this case the term d defined in (4.1) is very small at this local minimum point, and therefore d_{min}, the minimum value of d, is very close to 0. It happens that the term $\mathcal{R}_\gamma$ raises the value of d_{min}, essentially by pushing away, and actually up, the local minimum value from the threshold value. As a practical effect, the hole will not show up even at a higher perturbation of the threshold. Therefore, we greatly improve the topological stability of the reconstruction by adding the term $\mathcal{R}$.

Acknowledgment. The authors thank Hande Tüzel for providing the codes to compute the Hopkins aerial intensity.

REFERENCES

[1] L. AMBROSIO, N. FUSCO, AND D. PALLARA, *Functions of Bounded Variation and Free Discontinuity Problems*, Clarendon Press, Oxford, UK, 2000.
[2] S. K. CHOY, N. JIA, C. S. TONG, M. L. TANG, AND E. Y. LAM, *A robust computational algorithm for inverse photomask synthesis in optical projection lithography*, SIAM J. Imaging Sci., 5 (2012), pp. 625–651.
[3] N. COBB, *Fast Optical and Process Proximity Correction Algorithms for Integrated Circuit Manufacturing*, Ph.D. thesis, University of California Berkeley, Berkeley, 1998.
[4] G. DAL MASO, *An Introduction to Γ-convergence*, Birkhäuser, Boston, Basel, Berlin, 1993.
[5] X. MA AND G. R. ARCE, *Computational Lithography*, Wiley, Hoboken, NJ, 2010.
[6] L. MODICA, *The gradient theory of phase transitions and the minimal interface criterion*, Arch. Rational Mech. Anal., 98 (1987), pp. 123–142.
[7] L. MODICA AND S. MORTOLA, *Un esempio di Γ^--convergenza*, Boll. Un. Mat. Ital. B (5), 14 (1977), pp. 285–299.
[8] Y. C. PATI, A. A. GHAZANFARIAN, AND R. F. PEASE, *Exploiting structure in fast aerial image computation for integrated circuit patterns*, IEEE Trans. Semiconductor Manuf., 10 (1997), pp. 62–74.

[9] A. Poonawala and P. Milanfar, *Mask design for optical microlithography—an inverse imaging problem*, IEEE Trans. Image Process., 16 (2007), pp. 774–788.
[10] L. Rondi and F. Santosa, *Analysis of an inverse problem arising in photolithography*, Math. Models Methods Appl. Sci., 22 (2012), 1150026.
[11] F. Schellenberg, *A little light magic*, IEEE Spectrum, 40 (2003), pp. 34–39.
[12] V. H. Tüzel, *A Level Set Method for an Inverse Problem Arising in Photolithography*, Ph.D. thesis, University of Minnesota, Minneapolis, MN, 2009.